Materials Research Laboratory, Inc.

22333 Governors Highway ♦ Richton Park Illinois ♦ 60471
Pilgrim 8-8777 ♦ Chicago telephone ♦ PUllman 5-4020

FIRST INTERIM REPORT

on

ELEVATED TEMPERATURE STRESS CORROSION OF HIGH STRENGTH SHEET MATERIALS IN THE PRESENCE OF STRESS CONCENTRATORS

Contract NASr-50

for

Office of Research Grants and Contracts

Code BG

NATIONAL AERONAUTICS AND SPACE ADMINISTRATION
Washington 25, D. C.

November, 1964

by

R. L. Kirchner and E. J. Ripling

Materials
Research
Laboratory,
Inc.

ABSTRACT

Under laboratory creep furnace conditions, AM 350 stainless steels, Inconel W, and V-36 were unaffected by 1000 hr exposures at 650°F and 60 ksi in the presence of sea salt. Salt coated samples of the titanium alloys, Ti-6Al-4V and Ti-8Al-1Mo-1V, however, were found to be susceptible to stress corrosion cracking at 650°F and 17.5 ksi under the same creep furnace exposures. The average time to failure for the latter was about 240 hr; although two specimens survived the 1000 hr while one failed after only 23 hr. At 600°F, practically no deterioration was found in the titanium alloys after 1000 hours of exposure.

The severe sensitivity of titanium alloys to hot salt in laboratory tests is not consistent with its reported behavior in service. To be able to predict whether or not titanium is safe in specific applications requires a better understanding of the mechanism of hot salt stress corrosion cracking. Two experimental techniques have been developed for studying this phenomenon. The first of these used an elevated temperature oxygen concentration cell in which a salt bridge connected an air exposed titanium sample with a stressed one held at a reduced pressure. By this method, it was possible to measure the electrochemical characteristics of the corrosion. To supplement this, a tensile hot stage was used which made it possible to correlate the mobility of corrosion products with the cracking behavior.

On the basis of these observations, the following tentative mechanism for hot dry salt stress corrosion is proposed. The salt first dissolves the protective oxide layer on the titanium after which the salt reacts with the exposed metal to form a primary corrosion product. This primary product reacts with either oxygen or the water vapor in air to form a second solid which has a high rate of surface diffusion. The latter causes cracking as it creeps over the stressed metal surface.

CONCLUSIONS

PART I - SURVEY OF CANDIDATE MACH III SKIN MATERIALS

1. Under laboratory creep conditions, i.e., stagnant air and free of vibrations, the following alloys show no deterioration as a result of 1000 hr exposures at 650°F, at either 40 or 60 ksi in the presence of sea-salt: AM 350 20% reduced, aged 3 hr at 825°F; AM 350 20% reduced, aged 3 hr at 950°F; AM 350 45% reduced, aged 3 hr at 825°F; AM 350 45% reduced, aged 3 hr at 950°F; Inconel W 65% reduced, and V-36 30% reduced.

2. On exposure for 1000 hr at 850°F and 40 ksi, the two super-alloys, Inconel W 65% reduced, and V-36 30% reduced, suffered some property loss. The embrittlement, however, was found to result from a sensitivity to the stress concentrators and was not related to the presence of sea-salt.

3. The titanium alloys, Ti-6Al-4V and Ti-8Al-1Mo-1V, were found to be generally incapable of supporting stresses of 17.5 ksi for the 1000 hr exposure period at 650°F in the presence of sea-salt.

4. Temperature is a most important variable in stress corrosion cracking of titanium. At 600°F, the two titanium alloys exhibited little deterioration on exposure for 1000 hr at 25 ksi in the presence of sea-salt exposures, although some embrittlement was found in longitudinal samples of Ti-6Al-4V.

5. Stress level also contributes to the rate of stress corrosion cracking of Ti-6Al-4V and Ti-8Al-1Mo-1V. (The intimacy of contact of salt with the metal surfaces may be found to be more important than stress, however, and perhaps even more important than temperature.)

PART II - MECHANISM OF STRESS COSSOSION CRACKING IN TITANIUM ALLOYS

A number of experimental techniques have been applied to determining the mechanism of titanium-hot salt stress corrosion cracking. On the basis of these, the following observations were made:

1. Sodium chloride, ASTM salt (7 parts NaCl to one part $MgCl_2$), and sea-salt have significant conductivities at elevated temperatures, e.g., at temperatures in excess of 550°F. The corrosivity of the salts appears to be in order of their conductivity, NaCl being the least harmful and sea-salt being the most destructive.

2. Cracking occurs with heavy salt layers at the salt-metal-air interface.

3. Supplying an external voltage across the dry-salt layer on stressed titanium influences the time to failure and changes the position of crack initiation.

4. Slight differences in the availability of oxygen to salt covered titanium surfaces produce potential differences between oxygen deficient and air exposed areas.

5. It appears necessary to maintain intimate contact between the titanium and salt to cause corrosion. Vibrations that occur in service may prevent such contact and hence avoid stress corrosion cracking.

6. It is possible to generate the primary corrosion product at an elevated temperature and then produce cracking on subsequent room temperature storage under stress. If the corrosion product is washed off, cracking does not occur on subsequent storage. Possibly a secondary reaction that produces hydrogen and hence hydrogen embrittlement may be the cause of cracking.

7. The primary corrosion product does not cause cracking, or possibly even severe pitting in titanium. Although this product has not been identified, it reacts with water evolving a gas. Titanium monoxide which has been identified as a corrosion product (in only trace amounts) would react with water to evolve hydrogen, although hydrolysis of titanium chloride would also account for the observations.

8. A secondary product forms from the primary one presumably by a reaction with oxygen or water-vapor in the air.

9. Cracking appears to result during the formation of a secondary reaction product which is a solid that does not react with water.

10. The only reaction products identified by X-ray analysis are oxides of titanium and sodium chloride.

In summarizing these observations, the following tentative mechanism for hot-dry salt stress corrosion cracking of titanium is proposed:

A primary corrosion product is formed at the salt-titanium interface by the action of an oxygen concentration cell. This primary product reacts with oxygen or water-vapor in the air to form a secondary product which is a solid and causes cracking as it diffuses over the metal surface.

ACKNOWLEDGMENT

It is with a great deal of pleasure that the authors acknowledge the assistance and guidance given by Professor Herbert H. Uhlig of the Massachusetts Institute of Technology.

Materials Research Laboratory, Inc.

M R L

TABLE OF CONTENTS

Table of Contents, Continued

LIST OF TABLES

LIST OF ILLUSTRATIONS

List of Illustrations, Continued

List of Illustrations, Continued

List of Illustrations, Continued

List of Illustrations, Continued

INTRODUCTION

Because of the need for the greatest possible load carrying capacity per unit of weight, materials for the skin of supersonic transports must be used at the highest strength levels attainable for the particular class of alloys. In general, this requirement increases the susceptibility for stress corrosion cracking. Coupled with this is the need for long service life (30,000 hours), the ability to withstand thermal excursions from below 0 to 600°F, and resistance to corrosion in marine environments typical of airports near the ocean. Among the numerous material problems associated with this service requirement is a need for information on stress-corrosion cracking of the candidate materials, especially near the upper limit of this temperature range. The corroding medium of most concern is the sea-salt that is expected to accumulate on the aircraft because of the airport locations (1 - 3)*.

Three classes of materials were used in this study: (a) AM 350 series of stainless steels, (b) cold reduced superalloys (nickel and cobalt base), and (c) titanium base alloys.

The project was carried out as two reasonably independent phases. The first dealt with a creep exposure survey of the above listed materials. This portion of the work revealed that the titanium alloys, Ti-6Al-1V and Ti-8Al-1Mo-1V, were more susceptible to stress corrosion cracking in the presence of hot dry sea-salt (under laboratory testing conditions) than had previously been reported (4), Fig. 1. Other than its sensitivity to cracking in the presence of hot dry salt, the titanium alloys appeared to be the most promising of the candidate materials for the parts of the skin that do not become excessively hot. Consequently, it is essential to develop a better understanding of the mechanism of titanium hot dry salt stress corrosion cracking, and particularly to determine whether or not the severe cracking observed in laboratory tests under an essentially stagnant atmosphere is equivalent to service behaviors. Under actual service exposures, such variables as a moving air stream, variable pressure, and vibrations may either retard or accelerate. This mechanism study is discussed in Part II of this report.

---

* Numbers in parentheses refer to references at the end of this report.

PART I

SURVEY OF CANDIDATE SST SKIN MATERIALS

A screening program was undertaken to evaluate the susceptibility of candidate materials to stress corrosion cracking in the presence of hot dry salt. The screening process consisted of exposing salt coated notched and smooth tensile samples to stress at an elevated temperature for times of 1000 hr, or less if failure occurred during exposure. The samples that survived exposure were then tested at 650°F, room temperature, and -110°F, and the results compared with similar data on air exposed samples to evaluate the effect of the added dry salt.

MATERIALS AND TEST PROCEDURE

Materials

The materials used in the program were:

Stainless Steels	AM 350	20% reduced, aged at 825°F, 3 hr 20% reduced, aged at 950°F, 3 hr
	AM 350	45% reduced, aged at 825°F, 3 hr
Super alloys	Inconel W	65% reduced
	V-36	30% reduced
Titanium alloys	Ti-6Al-4V	annealed
	Ti-8Al-1Mo-1V	annealed

The materials were all supplied as sheets, nominally 25 mils thick, except for the Ti-8Al-1Mo-1V, which was approximately 20 mils. Their smooth tensile properties in the unexposed condition are shown in Table I.

Specimen Preparation

The sheets were sheared into the appropriate size coupons, and subsequently machined into ASTM edge notched or smooth specimens with the dimensions shown in Fig. 2. The notch radius of each sample was measured at 500 X, and all samples used for the exposure study had notch radii equal to approximately 0.00025 in.

The machined samples were washed in acetone to remove organic material, and were then thoroughly cleaned with Alconox in distilled water. Generally the specimens were allowed to soak in the Alconox solution for a few hours until water wet the surface with an essentially zero contact angle. After rinsing in distilled water and rewashing with acetone, the samples were dried and ready for salt coating.

The salt was obtained by evaporating natural sea water to a thick slurry which was applied to the specimens and then the excess water evaporated until only dry sea-salt remained on the samples. When coating notched specimens, care was taken to force the salt down into the base of the notch. A few of the notch samples were first coated on only one side and dried, after which they were examined from the reverse side to be certain that the salt was in contact with the notch bottom.

After coating, the specimens were loaded into the creep furnace stands. Three to six samples were placed in series, heated to the exposure temperature, and then loaded to the proper stress.

Exposure and Testing Procedure

Both longitudinal and transverse specimens of all of the above listed candidate materials were exposed for 1000 hr unless failure occurred sooner. Initially, the exposure conditions were 650°F and 40 ksi for the super alloys and stainless steels and 25 ksi for the titanium alloys. Both temperature and stress were subsequently increased for the super alloys and stainless steels until some property deterioration became apparent. For the titanium alloys, on the other hand, the initial exposure of 25 ksi and 650°F was found to be too severe, and subsequent tests were made at lower temperatures.

Samples of each series that survived exposure were tensile tested at 650°F, 75°F, and -110°F. The results were presented as notch-strength, and notch-strengh-ratio as a function of testing temperature for notch bars, and as tensile strength, yield strength and percent elongation vs. testing temperature for smooth bars. Test samples were not remachined after exposure, i.e., notched exposure samples were used for notch testing, etc. Property degradation was evaluated by comparing the salt exposure data with similar data obtained on air exposed sample.

Since the salt exposed titanium samples did not fracture across the notch plane where the stress was highest, a study was also made of the effect of exposure stress on this material at 650°F. For this test series, bend samples were used, and the stress levels varied from 0 to 40 ksi. The coupons were washed in the usual manner and then mounted on special bend racks, shown in Fig. 3. Unlike the creep exposure samples, the bend samples were stressed before the salt slurry was applied. After a bead of the slurry was dried on the center of the coupons, the racks were placed in a stainless steel box in order to attain a stagnant air atmosphere similar to that used in creep exposure. The exposure time was held constant at 100 hours. At the end of the exposure, the specimens were removed and machined to tensile samples for room temperature testing.

EXPOSURE RESULTS

Much of the air exposure data that was used for comparison with the salt exposed samples were taken from References (5) (6). In all cases, samples used for salt and air exposure were taken from the same heat. The notch-tensile strength of all samples that withstood the exposure are summarized in Table II.

Stainless Steels

Exposure to 40 ksi at 650°F for 1000 hr in the presence of heavy coats of sea-salt did not affect AM 350 stainless steels, 20 and 45% reduced, aged at 825°F or 30% reduced and aged at 950°F for 3 hr, Figs. 4 and 5.

To evaluate the influence of a higher stress, AM 350, 20% reduced, aged at 825° and at 950°F, were exposed under the same conditions of temperature, time and salt coating to 60 ksi. As shown in Fig. 6, no property loss resulted from the higher load sea-salt exposure.

Super Alloys

Comparison of the super alloys after dry sea-salt and air exposure to 40 ksi, 1000 hr, and 650°F showed that both Inconel W and the cobalt base alloy V-36 were unaffected by heavy salt coatings, Fig. 7. Increasing the exposure stress to 60 ksi did not damage Inconel W,

Fig. 8. On the other hand, 40 ksi and 100 hr salt exposure was damaging to the notch strength at 850°F, especially in the transverse direction, Fig. 9.

In order to determine whether the reduction in properties was due to the salt or merely to the increase in exposure temperature, both smooth and notched specimens were exposed to the same conditions in the absence of sea-salt. These test results are added to Fig. 9a. The air exposure tests indicated that the notch property losses were caused by the increased exposure temperature and could not be related to surface effects produced by the salt.

The results of exposing V-36 to dry sea-salt at 850°F and 40 ksi, Fig. 9b, were similar to those encountered with Inconel W. Again, the notch properties of the alloy were reduced as a result of the higher temperature creep exposure.

All of the notched stainless and superalloy samples fractured at the notch bottom. The steel and cobalt base alloys were stained by the salt layer, but the Inconel W was not, Fig. 10.

Titanium Alloys

Effect of exposure temperature - Salt coated longitudinal and transverse notched specimens of the titanium alloys Ti-6Al-4V and Ti-8Al-1Mo-1V were exposed at 650°F and 25 ksi. The planned exposure time was 1000 hours; however, most of the samples failed during exposure, and those that survived suffered serious property deterioration in subsequent tensile testing. Failures occurred anywhere from 23 to 975 hr of exposure, Table III. Although two transverse samples of Ti-8Al-1Mo-1V survived the exposure, one failed in 99 hours.

Surprisingly, fracture did not occur in the plane of the notch bottom where the nominal stress was 25 ksi (neglecting the stress concentrator of the 0.00025 inch radius notch). Instead failures occurred near the edge of the applied salt layer, Fig. 11, where the stress was only 70 percent of its maximum nominal value, i.e. 17.5 ksi. This sensitivity to cracking in the presence of sea-salt was greater than that reported for NaCl exposure (see Fig. 1).

On finding the severe susceptibility of the two titanium alloys to stress corrosion cracking, lower exposure temperatures were used to ascertain whether or not a threshold temperature existed for cracking at 25 ksi and 1000 hr.

Exposure studies were carried out for Ti-6Al-4V at 450, 500 and 600°F and on Ti-8Al-1Mo-1V at 500, 550 and 600°F for 1000 hr at 25 ksi. The post-exposure notch strengths of the alloys were compared with unexposed and 650°F air exposed data published by Syracuse University (5), and the Lewis Research Center (6), Fig. 12. The notch strengths of the salt exposed samples lie within the scatter band of the unexposed and air exposed specimens indicating that there is no embrittlement at 600°F and below for the stated stress and time. *

Smooth samples of both alloys were also exposed at 600°F for 1000 hours at 25 ksi, Table IV and Fig. 13. The tensile properties of Ti-6Al-4V were not affected by the exposure. (The tensile and yield strengths were lower and the elongation higher than that reported by Syracuse, but consistent with tensile data collected on unexposed samples at this laboratory, as shown in Fig. 13.)

Unlike the Ti-6Al-4V, the longitudinal samples of Ti-8Al-1Mo-1V suffered a severe loss in unnotched ductility after the 600°F exposure. This loss was not reflected in either the smooth tensile, yield, or in the notch strengths.

Effect of exposure stress - To evaluate the effect of stress, bend samples rather than tensile specimens were used in order to conserve creep capacity. Stainless steel racks of the type shown in Fig. 3 were made to provide four point loading of strip samples. The racks were designed to produce loads between 0 and 40 ksi. Each rack was calibrated at room temperature using foil strain gages on the tension and compression sides of titanium alloy samples.

---

* The edge of the salt coating applied to the 600°F exposure samples was made to coincide with the plane of the notch bottom in order to encourage cracking at this location. For the other samples, the salt was placed symmetrically about the notch.

The loaded specimen racks were placed in a stainless steel box for 100 hour exposures at 650°F. The box was used to more closely duplicate the stagnant atmosphere in a creep furnace. Tensile specimens of the type shown in Fig. 3 were machined from the exposed samples. The reduction in specimen width by machining assured the final testing of an area which had been subjected to a uniform stress during exposure.

No failures occurred in the course of the 100 hr exposures, although significant property deterioration did result, Table V and Fig. 14 and 15. Longitudinal samples of Ti-6Al-4V were only moderately damaged, but transverse samples suffered serious property losses in tensile strength and ductility. Ti-8Al-1Mo-1V was seriously damaged in both longitudinal and transverse directions, Fig. 15.

It is apparent from these results that stress is a significant factor in increasing alloy susceptibility, and if a threshold stress exists, it must be less than 10 ksi for the time and temperature selected. Since stress is an important variable, one would not expect the notch samples to fail at the edge of the salt layer, but at the plane of the notch bottom. Apparently the chemical reactions occurring at the salt-metal-air interface are capable of overriding the stress effect.

Further, on the basis of the creep exposure studies, one would have expected complete fracturing within the 100 hr for these bend specimens. The fact that this did not occur may be attributable to the fan motor being attached to the furnace in which these samples were exposed. This caused a modest vibration and salt was less adherent at the end of the test than was the case in creep testing.

PART II

MECHANISM OF STRESS CORROSION CRACKING IN TITANIUM ALLOYS

The severe sensitivity of titanium alloys to hot salt in laboratory tests is not consistent with its reported behavior in service. To be able to predict whether or not titanium is safe in specific applications requires a better understanding of the mechanism of hot salt stress corrosion cracking. This will not only lead to a more effective usage of the alloys but might also provide means for preventing or protecting against failures.

Because of the apparently conflicting statements that have been made on the elevated tempersture stress corrosion cracking of titanium alloys, studies carried out prior to this one are reviewed in chronological order in the appendix to this report. The conclusions most pertinent to the study are reviewed below.

EXPERIMENTAL STUDIES ON STRESS-CORROSION CRACKING

Reactants Necessary for Corrosion to Occur

General corrosion will take place with titanium and titanium alloys in the presence of hot,dry, alkali halides (7). The interaction of dry salt with titanium, however, requires a third ingredient (7) (4) (8) which can be oxygen or certain acidic oxides. Sodium chloride, for example, will react with titanium or titanium alloys in air to produce a corrosion product which is generally black, but the same product may be produced if Al_2O_3 is mixed with the salt and oxygen is excluded. Varying the partial pressure of oxygen from one-fifth to one atmosphere is not a significant variable in the general corrosion (8) and in stress corrosion cracking, failures may occur at pressures as low as 10 microns (9).

One percent chlorine in an ambient atmosphere will produce cracking in a hot dry system (8). Water vapor and hydrogen chloride do not affect elevated tempersture general corrosion (7), but their role is not yet clear in stress corrosion cracking.

Reaction Products and Reactions

The only reaction products that have been positively identified, and which were produced at temperatures from 600 to 800°F, are sodium chloride and oxides of titanium, although the presence of a small amount of chlorine and chlorides has been theorized. (ARF reported $TiCl_2$ when the eutectic mixture LiCl-KCl was used.) Sodium chloride may occur in the corrosion product either from diffusion or from chemical reactions via intermediate corrosion products. The final product generally includes a black substance which reacts with water vapor on cooling to form an acidic solution while giving off a gas. The following reactions would account for this behavior (8).

(1) $TiCl_2 + (x+1)\,H_2O = TiO \cdot xH_2O + 2\,HCl$

(2) $TiO + (x+1)\,H_2O = TiO_2 \cdot xH_2O = H_2$

The overall reaction involves the oxidation of Ti to form TiO_2, Ti_2O_3 and TiO (8) (10). Prior to the above reactions with the water vapor, titanium dioxide constitutes the bulk of the reaction product with the monoxide present in only trace amounts. The possible reactions and the corresponding free energies as a function of temperature are plotted in Figures 16, 17, 18, 19 and 20.

Physical Metallurgical and Chemical Effects

General corrosion is known to occur much faster in a fused salt system than in dry salt (11 - 14) and it has been suggested that at dry salt temperatures, a liquid consisting of low melting chlorides exists at the interface between the salt and metal surfaces, and that the amount of corrosion is proportional to the amount of fused salt present (15). Protective oxide films disperse into the overlying chloride salts (olid or liquid) to expose fresh surfaces to the effects of oxygen.

In order for corrosion to occur, there must be physical contact between the salt and the metal (7). Furthermore, corrosion products normally develop radially about the applied salt and their pattern is not influenced by air velocity. Attempts to produce eccentric patterns by passing air over corroding surfaces failed to do so, indicating that the reaction does not involve a gaseous attacking agent.

Service exposures are reported to be less severe than laboratory creep exposures (16) to the same conditions of stress and temperature in the presence of salt, indicating that moving air and/or vibrations and/or the amount of salt present may be important factors in controlling stress corrosion cracking.

Alloying elements are important in establishing sensitivity to cracking as shown by survey work done at Langley Research Center (17) and Douglas Aircraft Company (18). The following order of susceptibility has been indicated: Ti-4Al-3Mo-1V, Ti-13V-11Cr-3Al, Ti-6Al-4V, Ti-8Al 1Mo-1V, and Ti-5Al-2.5Sn.

STRESS CORROSION CRACKING THEORIES

On the basis of the experiments discussed above, several cracking mechanisms have been hypothesized. These may be categorized by the phase believed to be the attacking agent; all three phases, i.e., solid, liquid and gas, have been proposed.

Solid Chloride Salt Attack

Two mechanisms for cracking have been proposed in which the salt or reaction products may be solids. The first of these is an extension of the pyrosol formation proposed by M. E. Straumanis to explain embrittlement of titanium in the presence of fused halides. He suggests that oxygen may dissolve in the solid salt much as is the case for fused salt (19). The oxygen then migrates to the salt-metal interface and diffuses into the metal lattice which is expanded causing a reduction in its fracture stress.

In the second of the proposed mechanisms, the dry or hydrated salt serves as an electrolyte in an oxygen concentration cell with the tip of the crack being anodic to the metal surface or crack sides because of an oxygen deficiency at the crack bottom (20). For such a cell to remain operative, it is necessary for the electrolyte to remain in contact with the crack tip. Completion of the salt bridge (between anodic and cathodic surfaces) may be explained by (a) the fact that the corrosion products have a larger volume than the salt and hence are forced into the crack or (b) the salt or reaction products may have a high rate of surface diffusion and hence is able to creep along the walls of the developing crack.

Fused Chloride Attack

Both of the above mechanisms would be operative in a fused chloride system. The liquid phase would occur because of the suppression of the melting point of the salt layer adjacent to the metal surface due to the formation of eutectic mixtures of sodium and titanium chlorides. A corrosion cell involving a low melting reaction product that served as electrolyte was proposed by Crossley (15).

Gaseous Attack

The theory that chlorine or some other volatile product is formed which reacts directly with free titanium has been advanced in order to explain why stagnant air conditions seem to be more severe than moving air environments. The chlorine that is assumed to attack the grain boundaries is thought to be generated in the course of general corrosion.

PRELIMINARY STUDY OF ELECTROCHEMICAL CHARACTERISTICS OF STRESS CORROSION CRACKING

At the time that this project was undertaken the two most commonly discussed mechanisms for cracking were (a) the result of a gaseous attack and (b) the result of an oxygen concentration cell in which the crack tip was anodic to its sides. If the behavior were electrochemical, it is necessary (a) that the dry salt (or its liquid reaction product) be electrically conductive (b) that the cracking pattern be influenced by the application of an externally supplied voltage, and (c) that differential aeration would create a potential difference sufficient to maintain a deleterious current density. Tests were made to see if these requirements were satisfied. Additionally, some other experiments were carried out to study effects associated with electrochemical phenomena.

Conductivity Measurements of Dry Salt

Conductivity measurements were made as a function of temperature on three salts. The purpose of this was to determine whether or not dry sea-salt had a measurable conductivity in the vicinity of 600°F and also to compare the conductivity of natural sea-salt with synthetic (ASTM) sea-salt and sodium chloride as used by other investigators.

The conductivity cells consisted of a porcelain tube (3/8 in. long by 3/4 in. ID), and two discs of alloy separated by about 0.1 in. of salt, Fig. 21. Short bursts of dc current in the 0 to 50 μa range were used to calculate the resistivity of the salt. Care was taken not to introduce any significant polarization of the cell by reversing the current each tiem. The time of each run was controlled so that it took 50 minutes to bring the conductivity cells from room temperature to 1300°F. Standardizing of the time compensated for the temperature lag of the inner part of the cell, as well as any changes that might have occurred in the chemical composition of the salt in the heating process such as the loss of water or the diffusion of electrode oxide into the salt. Both V-36 and Ti 6Al-4V electrodes were used. The conductivities measured using the titanium electrodes with the sea-salt and ASTM salt were lower than those measured using the V-36 electrodes, Fig. 22.

It was found that sea-salt is considerably more conductive than either ASTM salt (7 parts NaCl to one part $MgCl_2$) or NaCl, the latter being the least conductive of the three.

In order to achieve a conductivity in ASTM salt comparable to that found in sea-salt at 650°F, the ASTM mixture must be heated to 725°F while the pure NaCl had to be heated to about 900°F. These temperature-conductivity-differences might account for the differences in the various salt exposed tensile results that have been reported.

Effect of Anodic and Cathodic Currents on Hot Dry Salt Samples

If cracking occurred at the edge of the salt layer rather than at the notch bottom because of the unique electrochemical characteristics at this location, it should be possible to move the fracture position in notched samples by developing a more uniform current flow through the entire salt coating. Hence, transverse samples of Ti-6Al-4V were exposed in which the applied salt layers were covered with titanium electrodes as shown in Fig. 23. Two samples were tested in this fashion. In both cases, approximately 20 μa of current per square inch was passed -- in one case using the sample as the anode and the other as the cathode. Both samples fractured near the plane of the notch bottom, as shown in Fig. 24, after very short exposure times. When the sample was made the anode, fracture occurred after 19.6 hr. and when it was the cathode, it occurred after 4.9 hr.

Effect of Differential Aeration on the Formation of an emf

A bend sample was submerged in a dry salt mixture containing 7 parts NaCl to 1 part $MgCl_2$ in an apparatus of the type shown schematically in Fig. 25. An unstressed coupon was then placed on top of the salt bed so that air was more accessible to it than to the buried specimen. The two samples were then connected with a nickel wire so that any potential difference which might result on heating could be measured. The difference in available oxygen did indeed create an emf between the two samples, and the voltage developed was proportional to the temperature of the apparatus. At 730°F, a potential of 0.25v was measured with a flow of electrons to the unstressed, air exposed members indicating that an oxygen concentration cell was possible in titanium salt corrosion.

After this experiment was repeated three times, a fourth experiment was run in which a piece of porous alumina satureated with salt, was placed between the two samples. This experiment was performed to see if a salt bridge could be maintained through a rigid member. The reason for the latter studies is discussed below.

CONTROLLED ATMOSPHERE EXPERIMENTS

Having shown that dry salts have measurable conductivity, that oxygen concentration cells can occur in a titanium-salt system, and the location of the fracture could be altered by an applied voltage, an apparatus was designed to carry out a more detailed study of the role of galvanic action and of oxygen in stress corrosion cracking.

Design

An apparatus was designed so that two stressed samples could be placed inside a test chamber in identical atmospheres, both specimens being in contact with one end of a salt bridge. The bridge extends from the inside of the chamber to the outside where physical contact of the salt is made with another air-exposed sample, Fig. 26. In the course of a test, a nickel wire connects one of the inside samples to the outside one so that the two form a closed circuit through the salt bridge. The inside neighboring, uncoupled sample serves as a control.

The chamber was constructed so that the inside could either be evacuated or filled with a given atmosphere while the outside sample was exposed to air. In order to achieve a reasonable vacuum within the cylinder, an alundum tube was glazed except for a small section, Fig. 27, which was saturated with salt. This salt-filled porous section served as the ionic bridge between the inner and outer samples.

Two flanged pyrex fittings were then attached to the ends of the alundum tube with an epoxy cement. The juncture was then covered with a silicone rubber compound to assure a vacuum tight seal. A photograph of the equipment is shown in Fig. 28.

When the chamber was evacuated, the inside coupled member, the salt bridge and the outside air exposed piece of titanium form an oxygen concentration cell that should simulate the oxygen deficient region (a) at the tip of a crack or (b) underneath a salt covered area.

Sea-Salt Experiments

Prior to performing the salt bridge tests with the alundum tube, a control experiment was run using a nonporous pyrex tube. Two samples, stressed to 120 ksi, were exposed to a pressure of 4 microns at 650°F for 100 hr. in the presence of sea-salt within the glass system. The purpose for this experiment was to reaffirm the need for oxygen in the corrosion reaction. At the end of the test, both samples were only slightly tarnished and showed no deterioration in tensile properties or ductility in subsequent tensile tests.

In the first series of experiments using the alundum tube with the salt bridge, the bend samples were placed in the apparatus in the manner described above, i.e., two identical bend samples in contact with the salt, one sample serving as a control and the other connected electrically to the outside sample. In every case, when the assembly was heated to 650°F, a potential developed with a flow of electrons from the inside to the outside indicating that the oxygen deficient samples were anodic to the outside coupon. The probable reactions were the oxidation of titanium inside the chamber, i.e., $Ti \rightarrow Ti^{++} + 2e$; and on the outside, where air is present, the reduction of oxygen, $1/2\ O_2 + 2e \rightarrow O^{=}$.

The primary purpose of these tests was to demonstrate that when a stressed sample was connected electrically to the outside sample

that it would crack, despite its evacuated environment, whereas the control sample, placed adjacent to the coupled sample in an identical environment would either not crack or at least show considerably less deterioration. Fig. 29 shows this difference between the coupled and uncoupled samples on removal from the corrosion cell.

The test as discussed above was repeated six times with reasonable success, and after this series the equipment was modified to make it possible to collect data on corrosion emf's and currents. The changes included the introduction of a flat section on the alundum tube, a variation in corrosion time, an internal heater, and a shorter salt bridge. The modified equipment did not yield consistent test results in that the coupled samples were not necessarily damaged more than the uncoupled ones. The cause for this was attributed to the high impedence of the salt bridge (10 to 20 megohms) and the fact that the pressure where the bend samples contacted the salt was considerable higher than that measured at the two ends of the cell. The high impedence limited the current flow even though an appreciable emf (0.25 to 0.35 volts) developed so that the additional corrosion of the coupled sample due to external coupling was modest. Further, the higher-than-measured pressure supplied sufficient oxygen for the uncoupled sample to corrode at a rate that was not much different from the coupled one.

The fact that corrosion is being controlled by local cells within the chamber rather than by current passage between the inside and outside air exposed sample can be shown by calculating the amount of corrosion product associated with the measured currents. Assuming a total measured corrosion current of 10μa-hours (a typical current volume) the weight of the corrosion product can be calculated according to Faraday's law as:

$$W = \frac{ItM}{nF}$$

where

W	=	weight in gm
I	=	current in amperes
t	=	time in seconds
M	=	atomic weight
n	=	change in valence of the metal
F	=	96,500 coulombs

The total weight of reacted metal, if it is assumed that titanium is basically the element going into the reaction, is about 9×10^{-6} gm. If the corrosion product were $TiCl_2$, it would decompose on exposure to air and would form TiO and/or TiO_2. The total weight of product, if TiO were the end product, for example, would be only approximately 2×10^{-6} gm. per sq. cm. The actual amount of corrosion product was many times this amount.

To avoid these problems, a dry salt was needed that had a higher conductivity than sea-salt. Ideally, it was also to have some characteristic that would make it possible to more effectively saturate the porous alundum so as to reduce the leak rate through the salt bridge. The lithium chloride-potassium chloride eutectic composition (53 w/o KCl - 47 w/o LiCl) was chosen for this purpose.

Lithium-Potassium Chloride Experiments

Both sea-salt and the above salt combination are primarily mixtures of alkali chlorides; however, the dry lithium-potassium chloride salt is about two orders of magnitude more conductive than dry sea-salt. Because of this additional conductivity, the current flow in the oxygen concentration cell and its effect on corrosion rates could be more easily studied. Further, the eutectic mixture had a much lower melting point than sea-salt, so that by super-heating the alundum prior to running the tests the salt was partially fused in the alumina pores which lowered the air leak rate through the salt bridge.

Early in the testing program it was necessary to evaluate the ability of alumina saturated with the lithium-potassium chloride mixture to prevent air passage in the cell. This was done by comparing the corrosion characteristic of samples exposed in a glass chamber with those exposed in the alumina chamber (see Test Nos. 1 and 2 in Table VI). Two bend samples (80 ksi) were placed on a salt encrusted piece of alumina inside of an evacuated pyrex tube for five hours. The temperature of one sample averaged 635°F and the other 650°F, and the exposure pressure was five microns. When these samples were removed at the completion of the test, their surfaces were completely untarnished. In the comparative test, two similarly bent samples were placed in contact with the salt bridge of the alumina tube. In this case, the exposure temperatures were 641 and 651°F. The exposure time was 15.8 hours and the pressure measured at the two ends of the chamber was 7×10^{-4}

millimeters Hg. Although both of these samples were not cracked on removal from the test chamber, they cracked shortly thereafter on exposure to air. Apparently the measured pressure of the two ends of the corrosion chamber is considerably lower than that immediately inside the salt bridge.

The fact that the samples were not broken on removal from the chamber but did fail within approximately twenty minutes after having coolded to room temperature implies that stress corrosion cracking occurs in several steps. The first stage involves the generation of a primary corrosion produce which requires the presence of a salt electrolyte. The second stage involves the reaction of this initial product with some component of the air (presumably oxygen or water vapor). Cracking*, then occurs either as a part of the reaction in which water vapor and/or oxygen enter as reactants or, as a subsequent effect of the formation of the secondary product. On the basis of this result, two additional series of samples (experiments 3 and 4 in Table VI) were exposed 15.5 and 14.5 hours at 650 and 620°F, again at a low pressure of 7×10^{-4}. Again on removing these specimens from the test chamber, they were found to be uncracked, but, again, these failed within twenty minutes after being held at room temperature in the test rack. These results indicate that under the exposure conditions of tests 2, 3 and 4, enough air is available within the chamber to develop the primary corrosion product at such a high rate that the addition of coupling to the outside air is not noticeable.

Separation of Primary Corrosion From Cracking

In an attempt to illustrate that cracking and the formation of primary corrosion product are two separate processes, Test No. 5 in Table VI was conducted. A reasonably high pressure (5×10^{-2} millimeters mercury) and temperature (655°F) were used to guarantee a significant amount of corrosion. After 13.5 hours of exposure, these samples were removed from the test chamber and one sample was rinsed with distilled water while both samples were under stress. After a few minutes the unwashed specimen cracked while the clean sample exhibited no property loss even after being held in the bend fixture for an additional twenty-four hours.

---

* The tendency to crack on subsequent air exposures also was noted in the use of sea-salt.

The reaction that causes cracking after the initial exposure can also occur in a reduced atmosphere. To demonstrate this, Test No. 6 was conducted under exposure conditions similar to Test Nos. 3 and 4 excepting at a much higher pressure (6×10^{-2}, instead of 7×10^{-4}). After twelve hours of exposure both of these samples cracked indicating that the secondary reaction involved in cracking can also occur at a somewhat reduced pressure.

Effect of Coupling to Air Exposed Sample

After having established the requirements to cause cracking in this system four tests (number 7, 8, 9 and 10) were conducted to evaluate the effect of coupling in developing the primary corrosion product. In this test series the salt bridge of the alumina tube was utilized to connect an inside bend sample, the anode, with the outside cathode. The exposure time was reduced from the normal 15 hours to 5 hours for this series, temperatures were maintained between 630 and 635°F and pressures between 3×10^{-3} and 7×10^{-4} millimeters Hg. In none of these test series were the samples cracked on removal from the exposure chamber. In three of the four studies, the coupled sample cracked within twenty minutes on subsequent air exposure while the uncoupled sample did not fail within twenty-four hours. In the fourth test (No. 7 in Table VI) neither the coupled nor uncoupled sample failed on 24 hour room temperature storage and the total current measured in this test series was the lowest of the four even though its generated emf was the highest within this series. Possibly the test pieces did not make good mechanical contact with the salt bridge. Nevertheless these tests show that the rate of formation of the primary corrosion product is accelerated by coupling to an air exposed sample, indicating that the primary corrosion product is the result of an oxygen concentration cell. The difference in oxygen pressure for the latter test series, of course, is supplied by the air exposure of the outside sample.

Effect of Fused Salt

One test was also conducted at a temperature above the eutectic point for the salt to compare the corrosion characteristics of a fused and dry salt (Test No. 11 in Table VI). For this test a pyrex tube was used instead of the corrosion cell so that the test results would be comparable with Test No. 1. At the higher temperature, but lower

pressure (compare Test 11 with 1) cracking occurred in a very short time even though the available oxygen in this test was considerably below that for any of the other tests conducted with the eutectic salt mixture. Obviously, a liquid is far more damaging than a solid salt. Even with the fused salt, the fracture occurred at the edge of the salt layer, Fig. 30.

DETECTION OF LIQUID IN HOT SALT-TITANIUM MIXTURES

Certain of the proposed mechanisms for hot salt stress corrosion cracking of titanium require that a liquid phase be present at the salt-titanium interface at temperatures in the vicinity of 650°F. Attempts to find such a liquid, however, have not been successful. To find the lowest temperature at which a liquid phase may occur, a series of mixtures of powdered titanium containing 6% aluminum powder and dried, ground sea-salt powder were prepared. The mixtures were heated in a Vycor tube until they fused and then were allowed to cool so that thermal arrest diagrams could be constructed. The lowest region of solid-plus-liquid was found at about 1100°F. While heating the mixtures, some bubbling occurred as low as 750°F. In order to determine whether volatile salts or a gas was being given off, a mixture of 50% (Ti-6Al)-50% sea-salt was heated to 2200°F again in a Vycor tube, but this time a smaller, heat-exchange tube was placed inside so the end of the water-cooled tube was about one inch from the top of the salt, Fig. 31. A volatile product did collect on the inner tube, but when examined in a hot stage microscope, it was found to have a melting point over 1000°F. The bubbling at the low temperature, therefore, must have been due to a gas, possibly water vapor. The test was repeated with a 1% (Ti-6Al)-99% sea-salt mixture with the same result.

This is in agreement with data collected by Braski and Heimerl (17) who have shown certain titanium alloys, including Ti-6Al-4V, to be susceptible to stress corrosion cracking at 550°F in the presence of pure sodium chloride. Since the melting point of the latter is 1473°F, it does not seem likely that a liquid exists at a temperature as low as 550°F.

TENSILE HOT STAGE EXPERIMENTS

In order to observe the relationship between the initiation of stress corrosion cracks and the corrosion reaction products, a constant

displacement, tensile hot stage was built. The equipment was designed so that it could be evacuated, or used with controlled atmospheres, such as purified argon, or dry or wet air, since these are thought to be important variables in stress corrosion cracking. The schematic drawing and photograph of Fig. 32 explain the operation of the stage.

Two types of tests were conducted with this equipment. In the first series a sample with dimensions as shown in Fig. 33 had a bead of salt slurry placed on the body of the sample so that the formation of cracks could be observed while the sample was held under load at temperature. In one test, the salt was placed on the side of the sample which was being viewed through the microscope, while on another test, the salt was placed on the back side of the test piece so that the crack and the primary corrosion products could be observed without interference from the unreacted salt. The purpose of the latter test was to watch the formation of a newly formed crack in order to determine whether or not a liquid phase was present. The results of these tests will be discussed later.

In most of the tests with this equipment, hooks were added to the two edges of the test sample as shown in Fig. 34a. When such a sample is loaded in tension, the hooks remain stress free. With this sample shape, a salt slurry was placed on the hook and the various reaction products migrated away from the salt bead in a manner determined by the physical form of the product. For example, if the cracking medium were a gas, one would expect cracks to initiate anywhere in area (A) shown in Fig. 24b. The extra finger marked "F" was added to the test sample so that the stress concentration would be symmetrical about the salt bead. Hence, if a stress concentrator encouraged cracking, a gaseous corrosion product would produce cracks with equal ease at points P_1 and P_2. Liquid or solid reaction products must diffuse along the surface of the arm to reach the stressed portion of the test sample. Consequently, if the cracking medium were a liquid or a solid, one would expect cracks to occur at the intersection of the hook and stressed body of the sample, point P_1.

A plastic model was made of the hooked sample, Fig. 35, in order to evaluate the stress concentration at the base of the prongs by photoelastic means. The prongs on the two sides of the sample were made so that on one a generous radius was provided, and on the other, the

junction points were as sharp as could be made in the cast plastic model. It is apparent from the series of pictures in Fig. 35 that the stress at the base of the filleted prong is no higher than in the body of the sample, whereas if the sharp prongs are used the heavily stressed volume of metal would be smaller than can be detected in this model. Nevertheless, it seems certain that the stress at points P_1 and P_2 are identical for either shaped prong.

Test Results on Hot Stage

In all of the tests carried out with the hot stage to date, the stage was open to the atmosphere. Because there was only one opening in the stage, the rate of air flow was minimal.

Location of crack initiation around salt - Prior to using the hooked samples, salt slurries were placed on the body of polished and etched test pieces. These samples were dried, heated and loaded as described above. Cracks began to form at the periphery of the salt bead, as shown in Fig. 36. Close examination showed a gray-brown reaction product surrounding the bead, and it was within this area that the cracks were initiated. The observation that cracks are initiated only at the salt-titanium-air interface with heavy coatings is consistent with the results previously reported on creep samples.

Diffusion of corrosion products - Ter tests have been made on samples with the side hooks. The migration of the corrosion products was recorded by lapse-time still color photography.

The appearance of a side hook at 25X in the Ti-8Al-1Mo-1V test sample is shown on the right-hand side of Fig. 37. The exposure stress on the piece was 50,000 psi. Immediately after the test sample reached 650°F, a light colored product (probably a thin film of salt) was found on the hook adjacent to the salt bead. Shortly after this a dark corrosion product formed at the edge of the salt and diffused along the length of hook eventually reaching the stressed portion of the sample. After reaching the stressed area, a crack formed in the titanium, as shown by the high magnification photomicrograph in the bottom right of this figure. In less than twenty-five hours, cracks had formed in both sides of the test sample at the junction of the hook and stressed body. The appearance of the sample at the completion of the test is shown in the bottom middle figure. The white dot in the middle of the sample is the control

thermocouple. The fact that cracking only occurred at this particular location indicates that the cracking medium is either a liquid or a solid that has a high rate of surface diffusion on titanium. The humidity within the hot stage during the course of this test was high, since water leaked onto the cold sides of the chamber.

Most of the testing done to date was on Ti-6Al-4V alloy. Because this material is somewhat less sensitive to hot salt stress corrosion than Ti-8Al-1Mo-1V alloy, the load for most of the tests was increased from 50,000 psi to 80,000 psi. (In a single test using a 50,000 psi stress, the cracking behavior was similar to that using the higher stress, but the size of the cracks in a limited time were so small they were difficult to find.) Other than the increased stress, the tests on the two alloys were identical. In all cases, the test was continued until some cracking was evidenced. The appearance of the metal in the vicinity of a hook for the Ti-6Al-4V alloy is shown on the left in Fig. 37. At 650°F, Ti-6Al-4V forms a gold oxide whereas Ti-8Al-1Mo-1V forms a blue oxide; however, the gas evolved as one of the corrosion products stains Ti-6Al-4V and changes it from gold to blue. As shown for very short times in Fig. 37, a blue stain forms elliptically about the salt bead. This stain grows, and within a few hours the breadth of the sample between the two hooks is completely blue, while the remainder of the sample is gold. As discussed above, if the corroding medium were gas, one would expect cracking to occur directly across from the center of the salt bead. In no case, however, were cracks found at this location. As corrosion continues, the dark corrosion product that formed on the Ti-8Al-1Mo-1V adjacent to the salt bead also formed on the Ti-6Al-4V alloy. Again, this reaction product diffuses along the length of the hook and onto the stressed body of the test piece. Eventually cracks are formed in this alloy at the junction of the hook and body of the sample. For the Ti-6Al-4V alloy, significant cracks required 60 to 240 hours and the dark corrosion product was found to cover a significant protion of the stressed member.

The appearance of the cracks and their location for the other Ti-6Al-4V alloy samples are shown in the photographs of Fig. 38. The photomicrograph on the bottom right shows that cracking is not always restricted to the grain boundaries, but follows certain crystallographic planes as well. Of course, the transgranular cracking may result because of the very largest exposure stress used in this study (80 ksi).

Physical form of cracking medium - Attempts to distort the interface of the dark corrosion product by means of a probe were unsuccessful, indicating that the surface diffusion product is a solid. Close examination of the reaction product also showed the formation of tiny fibers. These had a dendritic structure, further supporting the fact that the corrosion product is a solid with a high rate of surface diffusion.

To be certain that the cracking medium was a solid rather than a liquid, a single test was also conducted in which the salt slurry (a bead 5 to 10 mils in diameter) was placed on the side out of view of the microscope using a smooth tensile sample of Ti-6Al-4V alloy. Hence, the crack initiated on the reverse side of the sample and propagated through the specimen thickness and into the sight of the viewer.

Shortly after this test began a crack formed and propagated through the thickness of the specimen into sight. As the crack width increased the characteristic blue stain formed elliptically about the crack. Shortly afterward a smaller gray pattern developed around the center of the crack until a series of concentric ellipses delineated various thicknesses of corrosion product that had radiated from the salt bead. This corrosion product had the same appearance as the material with the high surface diffusion rate discussed above. The tip of the crack showed no concentration of corrosion product as would be expected if it were a liquid. When the heating element behind the specimen was brought up to a red glow, the inside of the crack could be readily observed and it appeared to be empty.

The experiment with the hooked sample discussed above showed that the corrosion product was either a solid or a liquid. The experiment now being described indicated it to be a solid or a gas, implying that it is, indeed, a solid. Liquid reaction products would tend to collect at the crack tip in an experiment of this type. To illustrate this phenomenon, the sample temperature in the above-mentioned experiment was raised to the vicinity of the melting point of sea-salt. As the sample was heated to 1120°F, a meniscus could be seen forming in the crack, while at the same time a volatile product was given off that clouded the quartz window of the hot stage. After maintaining the melting temperature for fifteen minutes and subsequently cooling the sample for examination, spots of salt were found at each crack tip proving that a liquid corrosion product would concentrate in the narrowest regions of a crack due to

capillary action. The appearance of this sample as a function of time is shown in Fig. 39. In conjunction with the fusion temperature experiments conducted in this study, it may be noted that Homorek and Herasymenko (21) have constructed a phase diagram for the titanium-sodium chloride system in which a eutectic point was found at 1121°F and 50 w/o Ti.

Characteristics of Solid Corrosion Product - On examining the metal under the salt bead in the tests with the hooked tensile samples, it was found that a significant amount of titanium reacted, as shown by the side and top view of the metal near the bead in Fig. 40. The surface under the salt had a high reflectivity. The reaction product under the unreacted salt was a black-caked material. When a drop of water was allowed to run across the sample it formed a low contact angle on the gray material that had the high rate of surface diffusion. It did not appear to dissolve the product or to react with it, however. The black product under the salt bead, on the other hand, reacted in the characteristic manner to pick up moisture and evolve a gas.

Effect of contact between salt and metal surface - It was noticed, as a by-product of several of the experiments, that the intimacy of contact between the salt and metal was important in developing the black corrosion product. This is expected if the formation of the primary corrosion product is the result of an oxygen concentration cell. In several tests the salt bead on the arm of the sample was jarred with a pointer. The subsequent formation of primary corrosion product was almost imperceptible. Upsetting the salt may have destroyed the oxygen concentration gradient needed to produce the primary product. In one test, a piece of salt was knocked off the prong and became fastened electrostatically to the main body of the sample. In this latter case, no corrosion product formed at all, even after two days of exposure.

ANALYTICAL STUDY

A preliminary study was also made of an electron microprobe analysis of the metal near a crack tip, and an X-ray analysis of corrosion products.

Electron Microprobe

In an electron probe study conducted at the North American Aviation (22), it appeared that the crack followed the regions of concentration of high-atomic-number alloying elements, viz. molybdenum. An attempt was made at this laboratory to reproduce these results. Fig. 41a is an electron image of the area at a crack tip and is similar to a light photograph as viewed with oblique illumination. Figures 41b, c and d are molybdenum, aluminum, and vanadium X-ray images of the same areas at the same magnification as shown in Fig. 41a*. The brightness of an area is proportional to the amount of the element present. There does appear to be bands of Mo, Fig. 41b, however these do not seem to lie in definite paths which would be taken as corrosion routes.

X-ray Analysis

For the purposes of analyzing the corrosion product, Ti-6Al-4V coupons were heated to 650 to 700°F with a sea salt coating and held at temperature in the absence of load for 287 hours. The samples were then removed from the furnace and placed in a desiccator which was subsequently purged with argon. The desiccator was placed in a dry box where the corrosion products were scraped off of the samples and placed in capillary tubes. Care was taken not to collect any of the unreacted salt.

An X-ray analysis of the corrosion product showed the major constituents to be TiO_2 (anatase) and NaCl. The minor constituents were TiO_2 (rutile), Ti_2O_3, and TiO. The identification of TiO was reported as tentative, but it is the only compound reported (assuming $TiCl_2$ to be absent) that can explain the hygroscopic behavior of the black corrosion product that evolves a gas, presumably hydrogen, on picking up moisture.

It must be mentioned that titanium chlorides may still be considered to be important ingredients in the corrosion reactions even though they are not found in the analysis. In the proposed reactions, chlorides are continuously being formed and reacting so that they may be present only in small quantities.

---

* The electron microprobe photographs were made by IITRI.

TABLE I

SMOOTH TENSILE PROPERTIES OF THE UNEXPOSED TEST MATERIALS AT ROOM TEMPERATURE*

Alloy	Cold Work Percent	Age Time Hours	Age Temp °F	Longitudinal T.S. 1000 psi	Longitudinal Y.S. 1000 psi	Longitudinal e Percent	Transverse T.S. 1000 psi	Transverse Y.S. 1000 psi	Transverse e Percent
AM 350	45	3	825	278.5	277	2.5	279.5	266	3
AM 350	45	3	950	242.5	239.5	2.5	249	241	3
AM 350	20	3	825						
AM 350	20	3	950	184.5	174.5	18.5	195	171	16.5
V 36	30	0	0	219.5	200.5	6	222	193.7	7
Inc. W	65	0	0	192	184	3	184.5	167	4
Ti-6Al-4V	(Annealed)			147	140.5	11	153	145	12.5
Ti-8Al-1Mo-1V	(Annealed)			139.8	135.2	21	140.8	136.8	19

* All specimens tested were made from sheet material 0.025 in. thick, with the exception of the Ti-8Al-1Mo-1V which was 0.018 in. thick.

TABLE II

POST EXPOSURE NOTCH-TENSILE STRENGTH
OF CANDIDATE SST MATERIAL

ALLOY	EXPOSURE	-110 Long.	-110 Trans.	R. T. Long.	R. T. Trans.	+650 Long.	+650 Trans.
Inc. W-65% Red.	850 F, 40KSI	196.7	187.0	193.9	159.8	153.8	116.7
		209.4				175.1	
	650 F, 40KSI	222.4	221.0	200.0	199.0	171.6	173.0
			211.0	209.0	193.0	171.4	172.0
	650 F, 60KSI	220.0	212.7	208.0	200.0	182.2	166.0
V-36 - 30% Red.	650 F, 40KSI	182.6	140.2	179.4	164.4	143.2	129.2
		198.3		188.0	170.0	153.7	141.0
AM350 - 20% Red., 825 F, 3 hr	650 F, 40KSI	224.0	197.2	212.9	204.4	160.0	152.0
		219.5	206.0	212.0	205.0	172.9	148.8
	650 F, 60KSI	223.0	209.9	215.0	201.0	166.1	143.3
AM350 - 20% Red., 950 F, 3 hr	650 F, 40KSI	219.0	187.2	187.9	198.0	166.0	152.0
		197.8	186.6	188.0	181.0	152.9	133.2
	650 F, 60KSI	195.2	181.2	223.0	191.5	151.8	130.3
AM350 - 45% Red., 825 F, 3 hr	650 F, 40KSI	295	212	281.6	221.0	146.3	129.2
AM350 - 45% Red., 950 F, 3 hr	650 F, 40KSI	302	222.0	251.4	228.7	161.6	124.9
		264.4		240.8		179.0	
AM367 - 45% Red., 950 F, 4 hr	650 F, 40KSI	71.3	65.4	167.0	63.0	238.5	
Ti-6Al-4V, Annealed	450 F, 25KSI	138.2			125.0		112.8
	500 F, 25KSI	138.4	145.2	126.4	131.9	102.2	
		147.0					
	600 F, 25KSI*	157.4	145.5	128.8	137.2	103.8	114.5
		128.0	144.8	133.0	132.8	102.1	113.8
Ti-8Al-1Mo-1 V, Annealed	500 F, 25KSI	122.8	128.8	125.4	131.2	109.1	103.6
		106.1	127.2	120.1	120.4	109.5	101.8
	550 F, 25KSI	122.0		120.4			100.8
	600 F, 25KSI*	107.3	128.8	106.8	129.8	109.9	102.4
		101.8	131.9	118.0	123.6	110.4	103.0

* Exposed at 550°F for 215 hours and raised to 600°F for 1000 hours.

TABLE III

CREEP FURNACE SURVIVAL TIMES FOR Ti-6Al-4V and Ti-8Al-1Mo-1V

ALLOY	EXPOSURE	Time to failure, hr	
		Long.	Trans.
Ti-6A-4V, annealed	650°F, 25KSI	63	23
		187	276
			394
			975
Ti-8Al-1Mo-1V, annealed		120	99
		240	Two trans. samples
		283	la. d 1000 hr
			one tested .t -110°F
			had T. S. = 32. 3 KSI
			one tested at +650°F
			had T. S. = 58. 2 KSI

TABLE IV

POST-EXPOSURE SMOOTH TENSILE PROPERTIES
OF SALT COATED TITANIUM

Exposure Condition: 1000 Hr at 600°F, 25 KSI *

	LONGITUDINAL			TRANSVERSE		
Alloy	Tensile Strength	Yield Strength	Elonga.	Tensile Strength	Yield Strength	Elonga.
Ti-6Al-4V						
- 110	178.5	161.0	4	173.5	165.0	--
R. T.	140.0	133.9	9	152.0	144.6	12
+ 650				99.9	95.6	9
Ti-8Al-1Mo-1V						
- 110	150.5	150.5	2	169.5	144.5	20.5
R. T.	134.7	134.7	[illegible]	141.8	136.1	17
+ 650				87.8	85.5	3

* These samples were at 550°F for 215 hrs. and then raised to 600°F for 1000 hrs.

TABLE V

Ti-6Al-4V (LONGITUDINAL)

Smooth tensile properties of salt coated bend specimens.
0.025 in. thick specimens on 4-point load racks, 100 hr tests.

Exposure Stress KSI	Tensile Strength KSI	Yield Strength KSI	e percent	
37.2	147.8	-	7	Salt on tension side
7.6	151.0	144.5	13	" " " "
7.5	-	-	-	" " " "
7.6	149.9	140.7	13	" " " "
21.8	144.8	139.6	12	" " " "
21.8	-	-	-	" " " "
21.8	148.4	141.8	11	" " " "
36.7	-	-	-	" " " "
36.0	146.2	138.4	8	" " " "
0.0	145.8	132.0	11	" " " "
0.0	148.6	138.6	11	" " " "
0.0	148.7	139.1	12	" " " "
36.2	148.7	138.6	10	" " compression side
36.2	148.0	137.1	11	" " " "
0.0	148.6	139.1	11.5	no salt, same gaseous atmos. as above specimens
0.0	149.6	137.3	11.5	no salt, same gaseous atmos. as above specimens

TABLE V (cont.)

Ti-6Al-4V (TRANSVERSE)

Smooth tensile properties of salt coated bend specimens.
0.025 in. thick specimens on 4-point load racks, 100 hr tests.

Exposure Stress KSI	Tensile Strength KSI	Yield Strength KSI	e percent	
7.7	157.8	-	14.0	Salt on tension side
23.8	148.0	-	2	" " " "
7.7	154.6	-	13	" " " "
7.7	153.0	-	14	" " " "
24.0	153.0	-	8	" " " "
24.0	153.0	-	8	" " " "
40.1	105.9	-	1	" " " "
39.8	132.8	-	1	" " " "
40.0	104.7	-	2	" " " "
0.0	155.2	144.8	14	" " " "
0.0	155.7	144.9	15	" " " "
0.0	157.0	150.0	14	" " " "
38.8	150.2	145.0	14	" " compression side
38.8	155.3	146.0	14	" " " "
0.0	156.6	147.0	14	No salt, same gaseous atmos. as above specimens
0.0	156.8	149.1	13.5	No salt, same gaseous atmos. as above specimens

TABLE V (cont.)

Ti-8Al-1Mo-1V (LONGITUDINAL)

Smooth tensile properties of salt coated bend specimens.
0.018 in. thick specimens on 4-point load racks. 100 hr tests.

Exposure Stress KSI	Tensile Strength KSI	Yield Strength KSI	e percent	
17.7	137.9	137.9	3	Salt on tension side
28.8	80.4	-	1	" " " "
0.0	146.8	141.9	20	" " " "
0.0	148.1	-	18	" " " "
5.6	148.0	-	11.5	" " " "
5.5	146.8	-	20.5	" " " "
5.5	144.2	-	16.5	" " " "
17.5	126.8	-	2	" " " "
17.5	132.9	-	1	" " " "
28.5	82.5	-	1	" " " "
29.2	107.0	-	1.5	" " " "
28.5	148.5	141.9	19	" " compression side
28.0	145.2	141.4	19.5	" " " "
0.0	145.0	139.9	19	No salt, same gaseous atmos. as above specimens.

TABLE V (cont.)

Ti-8Al-1Mo-1V (TRANSVERSE)

Smooth tensile properties of salt coated bend specimens.
0.018 in. specimens on 4-point load racks, 100 hr test.

Exposure Stress KSI	Tensile Strength KSI	Yield Strength KSI	e percent	
5.7	131.0	-	14	Salt on tension side
0.0	146.0	140.0	14	" " " "
0.0	144.9	139.8	17	" " " "
5.8	144.2	140.8	17	" " " "
18.3	119.0	-	2	" " " "
18.0	108.4	-	2	" " " "
29.6	125.8	-	1.5	" " " "
29.7	132.7	131.1	1.5	" " " "
29.2	131.8	-	2.5	" " " "
29.2	143.2	139.1	16	" " compression side
28.8	141.0	140.8	17	" " " "
0.0	141.1	137.0	-	No salt, same gaseous atmos. (air and reaction products) as above specimens.
0.0	144.1	140.0	16	No salt, same gaseous atmos. (air and reaction products) as above specimens.

TABLE VI

RESULTS OF CORROSION CELL EXPERIMENTS USING LiCl-KCl EUTECTIC MIXTURE FOR THE ELECTROLYTE

All Samples Were 1 x 6 in. Transverse Coupons of Ti-6Al-4V, Stressed to 80 ksi By Bending

Test No.	Test Time	Coupled	Uncoupled	(°F) Temp.	(mm Hg) Pressure	(μa-hr) Total Current	(v) Ave. emf.	No Cracks On Removal	Cracked During Test	Broke on Exposure to Atmos.	Survived Exposure to Atmos.
1	5.1		x	650	$5x10^{-3}$	0	0	x			x
	5.1		x	635	$5x10^{-3}$	0	0	x			x
2	15.8		x	651	$7x10^{-4}$	0	0	x		x	
	15.8		x	641	$7x10^{-4}$	0	0	x		x	
3	15.5	x		651	$7x10^{-4}$	80	0.5	x		x	
	15.5		x	653	$7x10^{-4}$	0	0	x		x	
4	14.5	x		620	$7x10^{-4}$	11.8	0.4	x		x	
	14.5		x	620	$7x10^{-4}$	0	0	x		x	
5	13.5		x	655	$5x10^{-2}$	0	0	x		x	
	13.5		x	655	$5x10^{-2}$	0	0	x			x
6	12.0		x	660	$6x10^{-2}$	0	0		x		
	12.0		x	658	$6x10^{-2}$	0	0		x		
7	5.0		x	635	$6x10^{-4}$	0	0	x			x
	5.0	x		630	$6x10^{-4}$	5.5	1.1	x			x
8	5.1		x	636	$6x10^{-4}$	0	0	x			x
	5.1	x		633	$6x10^{-4}$	17.5	0.9	x		x	
9	5.1	x		630	$3x10^{-3}$	13	1.0	x		x	
	5.1		x	633	$3x10^{-3}$	0	0	x			x
10	5.1	x		635	$7x10^{-4}$	8.6	0.6	x		x	
	5.1		x	634	$7x10^{-4}$	0	0	x			x
11	0.5		x	690	$5x10^{-5}$	0	0		x		
	1.5		x	690	$5x10^{-5}$	0	0		x		

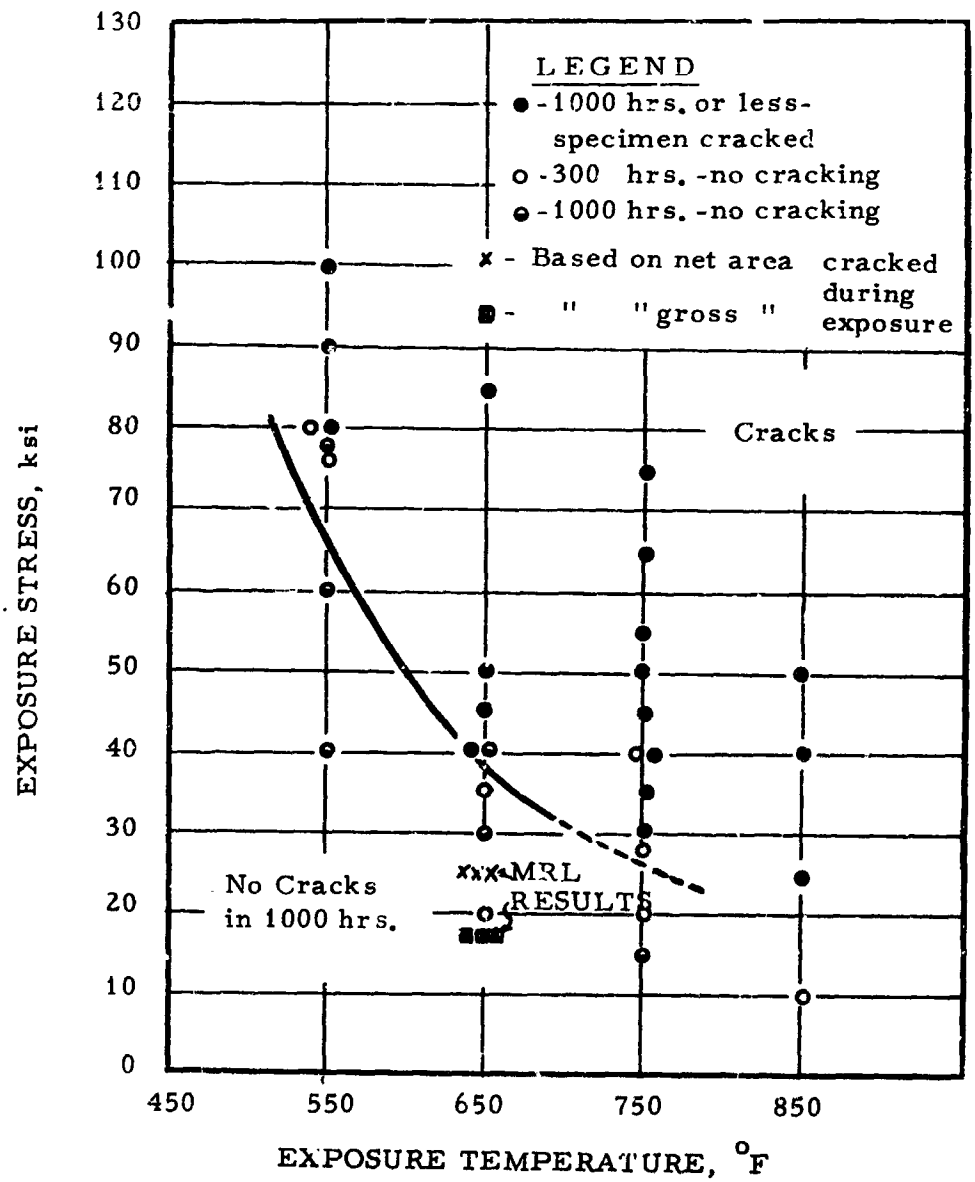

Fig. 1 EXPOSURE STRESS TO CAUSE CRACKING AT TEMPERATURES BETWEEN 550 AND 850°F AS REPORTED IN THE LITERATURE (4) COMPARED WITH MRL RESULTS. ANNEALED Ti-6Al-4V.

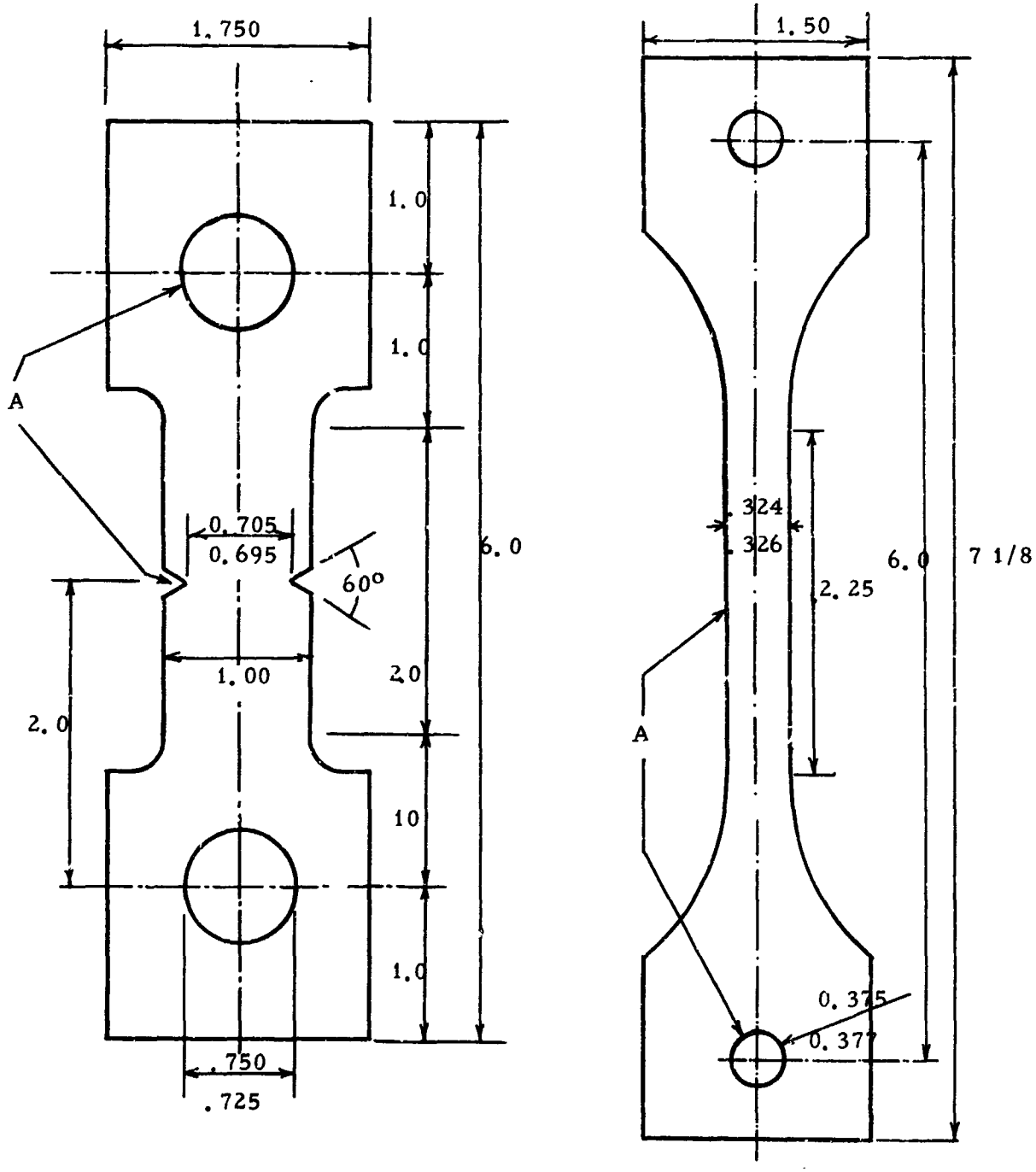

A - Surfaces true to centerline within 0.001 inch
Notch root radius less than 0.001 inch.

Fig. 2 NOTCH AND SMOOTH TENSILE SPECIMENS.

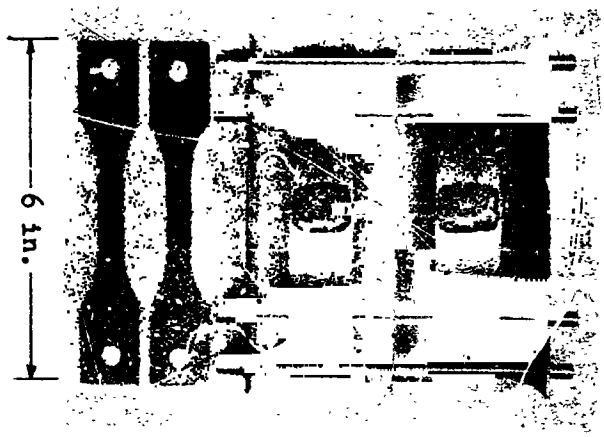

Fig. 3 SALT COATED BEND SPECIMENS MOUNTED ON TEST RACK (right) AND BEND SPECIMENS CUT DOWN TO TENSILE SPECIMEN SHAPE (left).

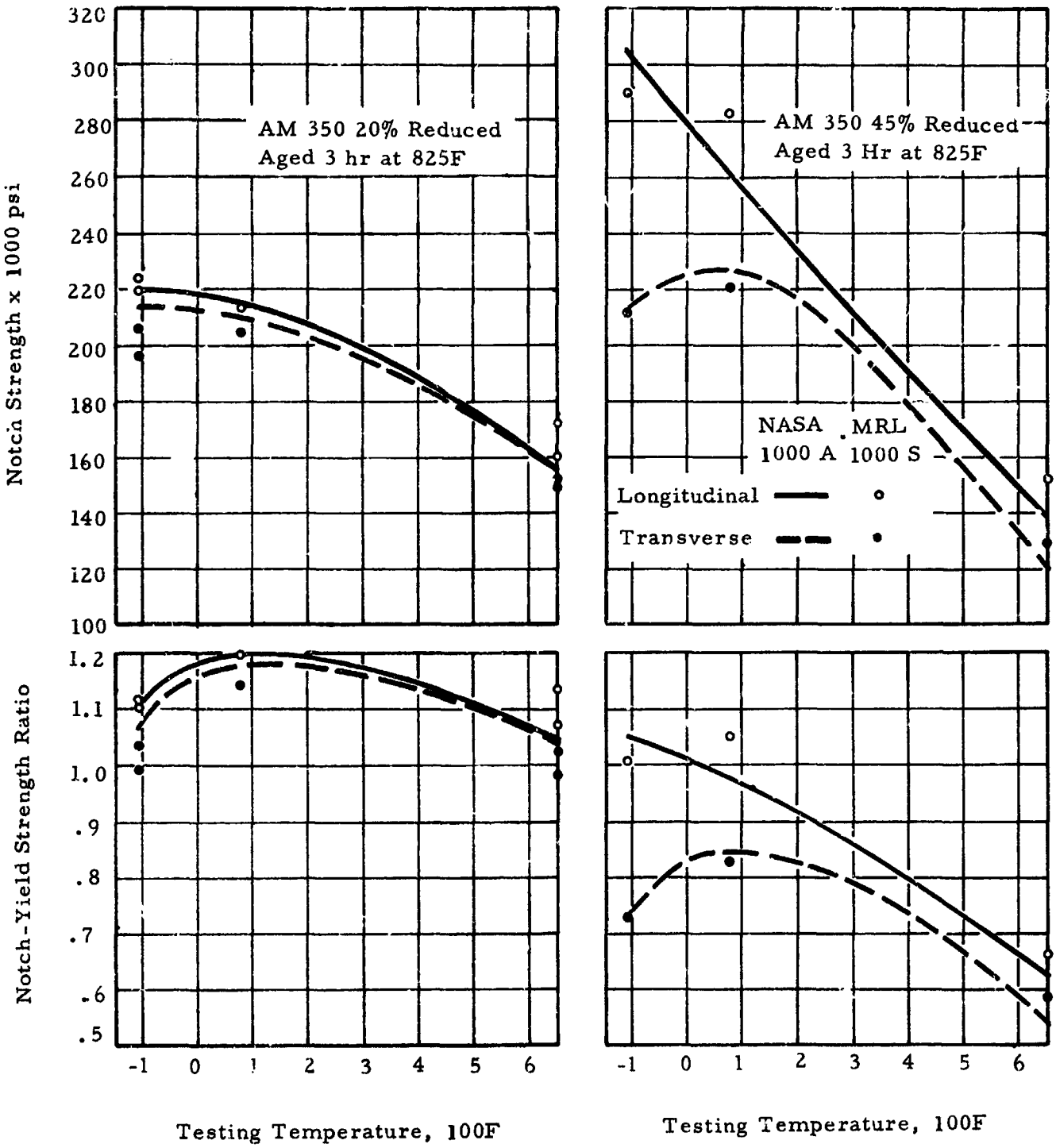

FIG. 4 COMPARISON OF AIR AND DRY SEA SALT EXPOSURE ON THE NOTCH PROPERTIES OF AM 350, REDUCED 20 AND 45%, AGED 3 HR 825F. ALL SAMPLES EXPOSED FOR 1000 HRS AT 650F AND 40,000 psi.

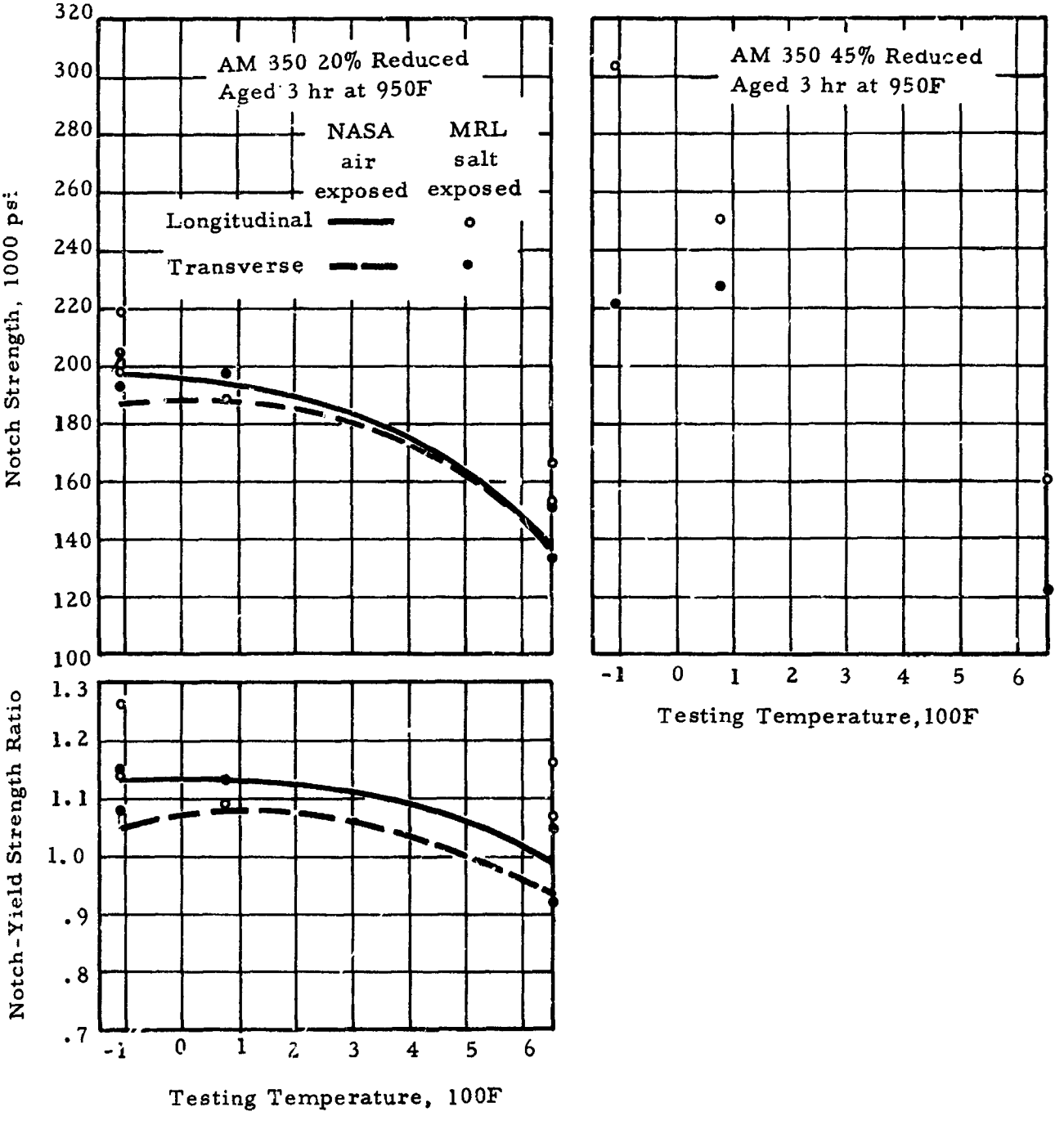

FIG. 5 COMPARISON OF AIR AND DRY SEA SALT EXPOSURE ON THE NOTCH PROPERTIES OF AM 350, REDUCED 20 AND 45%, AGED 3 HR 825F. ALL SAMPLES EXPOSED FOR 1000 HR AT 650F AND 40,000 psi PRIOR TO TESTING.

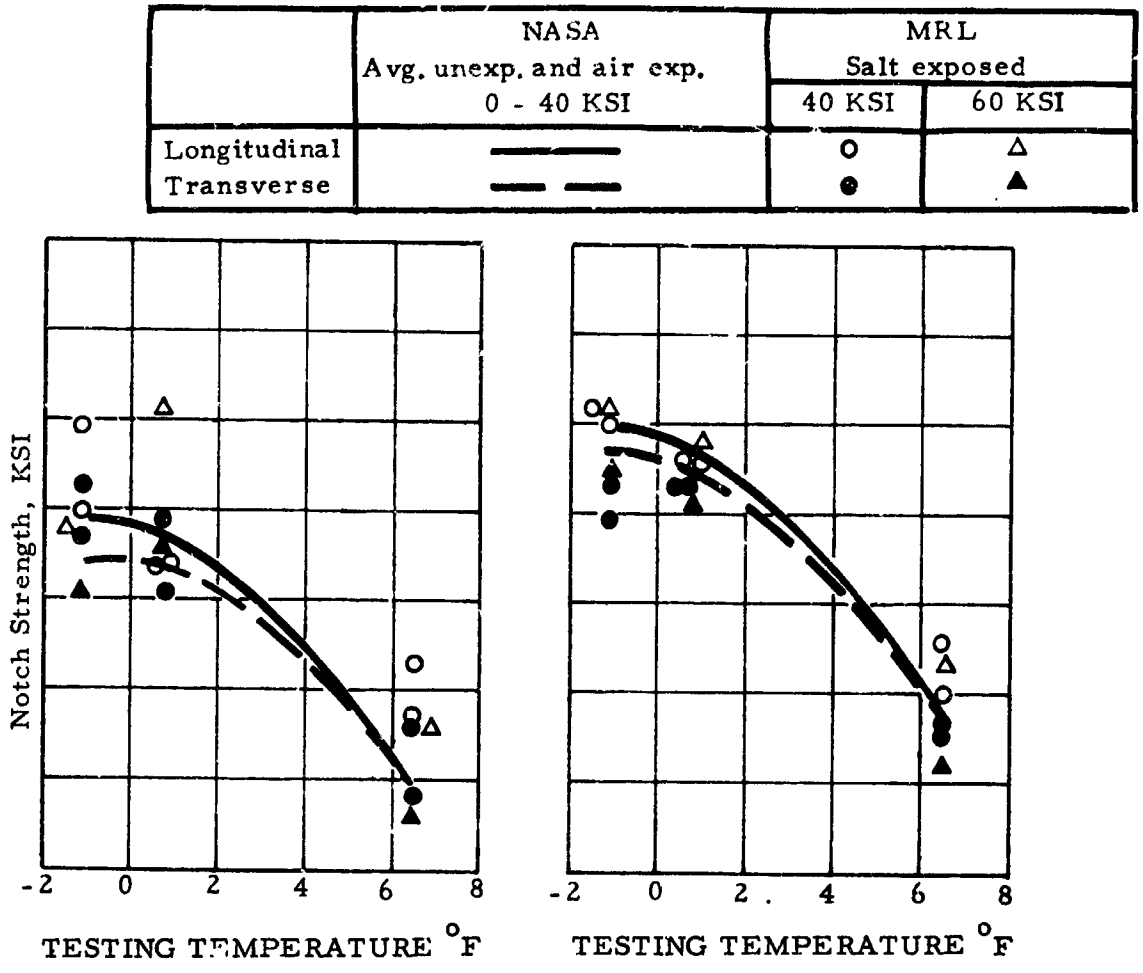

(a) AM 350, 20% reduced
Aged 950°F, 3 hr

(b) AM 350, 20% reduced
Aged 825°F, 3 hr

Fig. 6 EFFECT OF EXPOSURE STRESS ON NOTCH STRENGTH OF SALT COATED SPECIMENS OF (a) AM 350, 20% REDUCED, AGED 950°F, 3 HR, AND (b) AM 350, 20% REDUCED, AGED 825°F FOR 1000 HR AT INDICATED STRESS LEVEL.

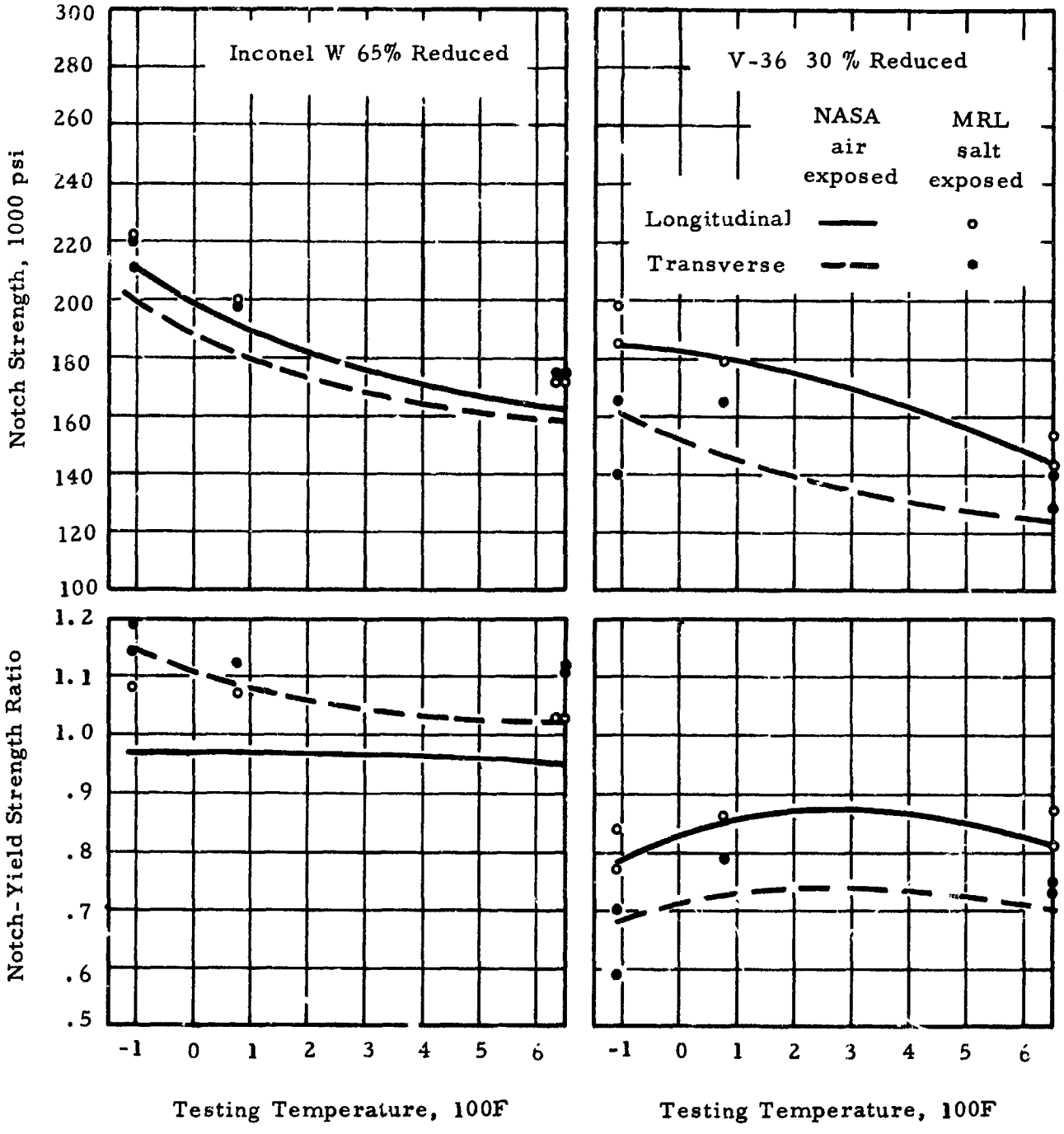

FIG. 7 COMPARISON OF AIR AND DRY SEA SALT EXPOSURE ON THE NOTCH PROPERTIES OF INCONEL W AND V-36. ALL SAMPLES EXPOSED 1000 HR AT 650F AND 40,000 psi PRIOR TO TESTING

	NASA Avg. unexp. and air exp. 0 - 40 KSI	MRL Salt exposed	
		40 KSI	60 KSI
Longitudinal	———	○	△
Transverse	— —	●	▲

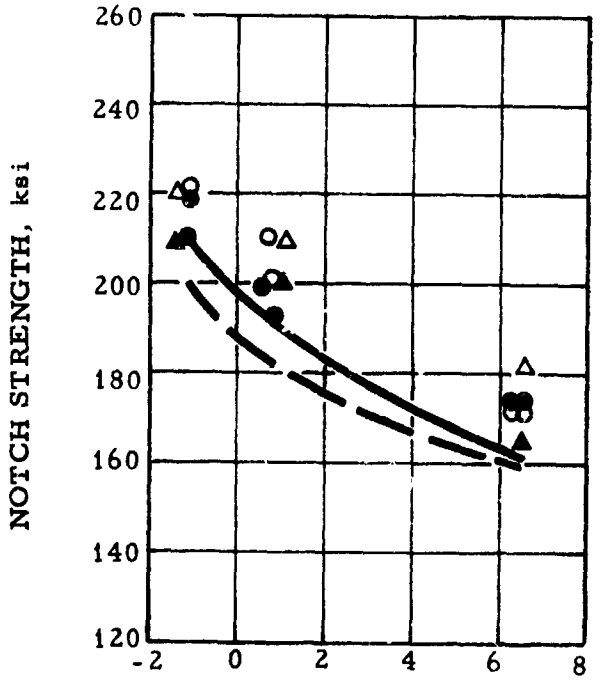

Fig. 8 EFFECT OF INCREASED EXPOSURE STRESS ON NOTCH STRENGTH OF SALT COATED INCONEL W, 65% REDUCED, EXPOSED AT 650°F FOR 1000 HR AT THE INDICATED STRESS LEVEL.

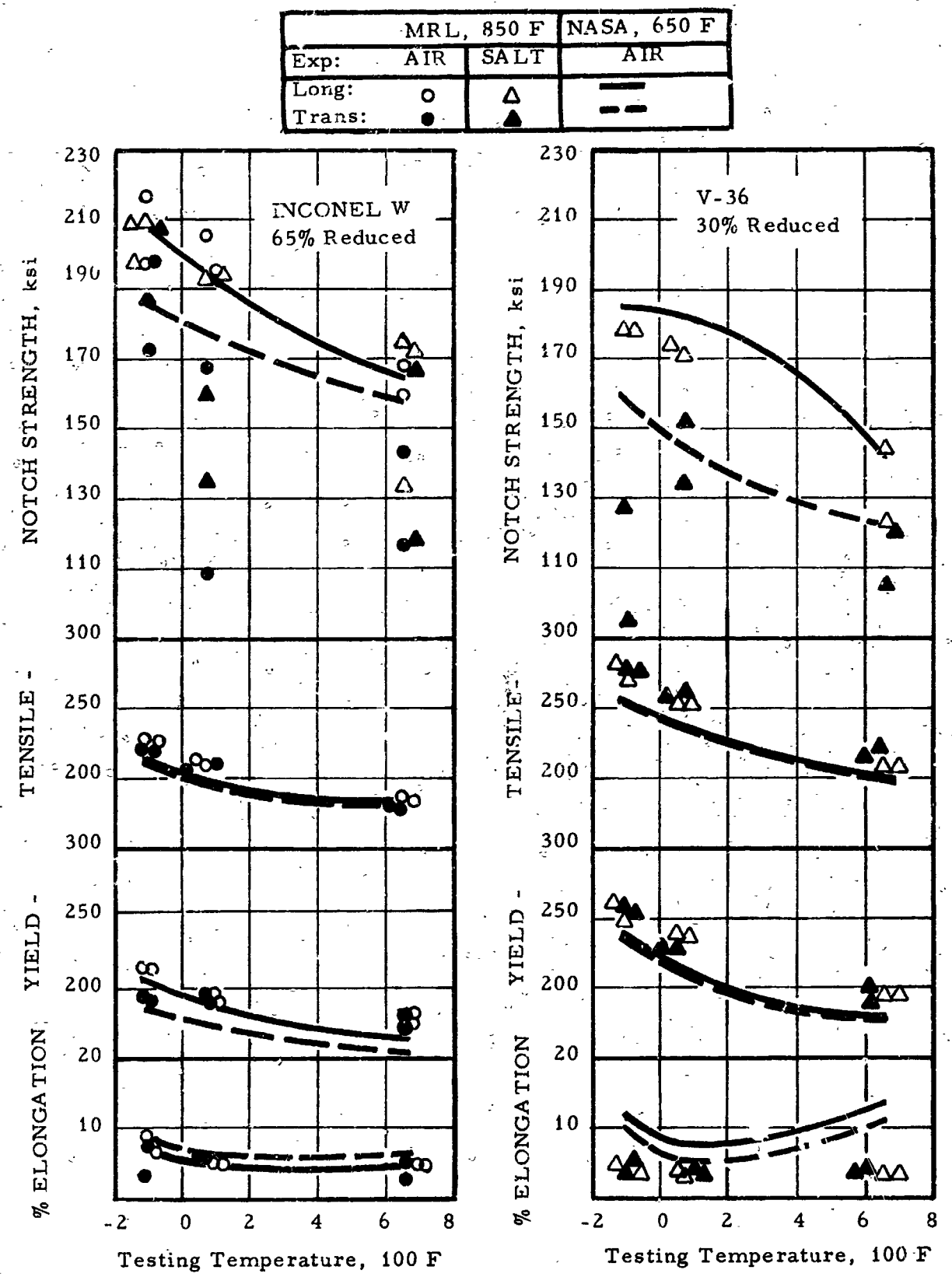

Fig 9a EFFECT OF SALT AND AIR EXPOSURES AT 850 F, 40ksi, 1000 hr ON SMOOTH AND NOTCHED SAMPLES OF INCONEL W

Fig.9b EFFECT OF SALT EXPOSURES AT 850 F, 40ksi, 1000 hr ON SMOOTH AND NOTCHED SAMPLES OF V-36

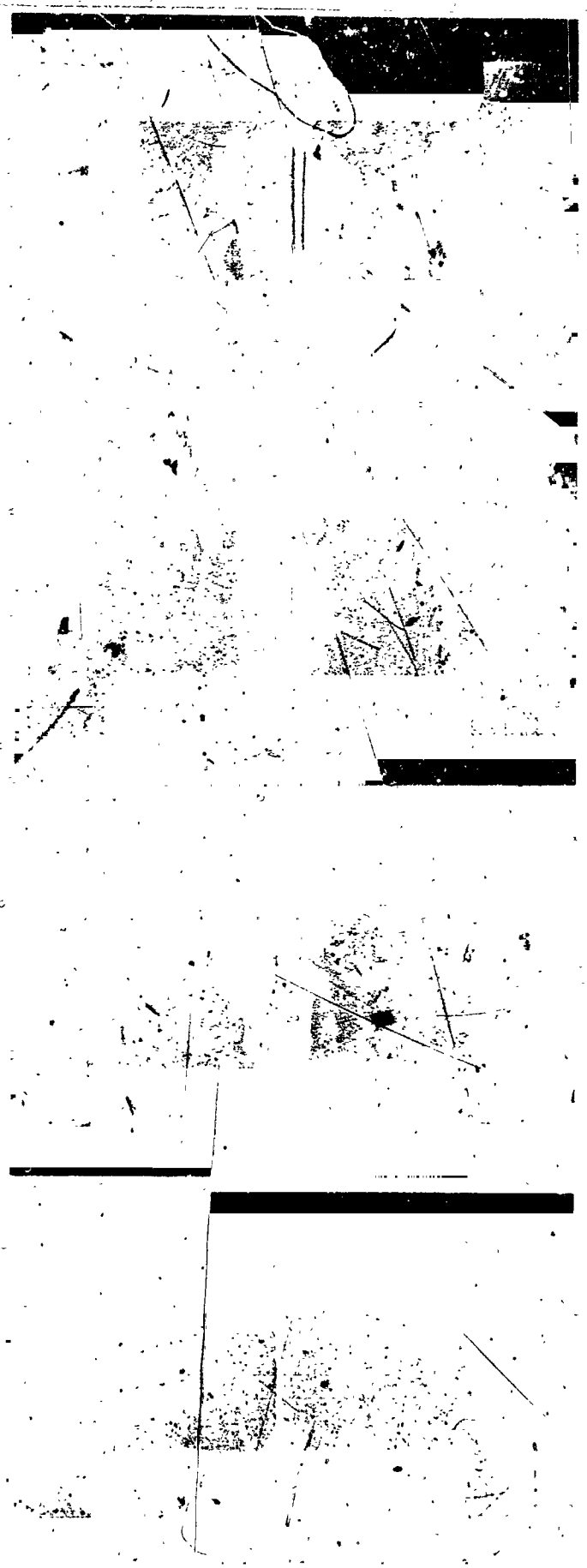

Fig. 10 SURFACE APPEARANCE OF EXPOSED SPECIMENS AFTER SUBSEQUENT TENSILE TEST.

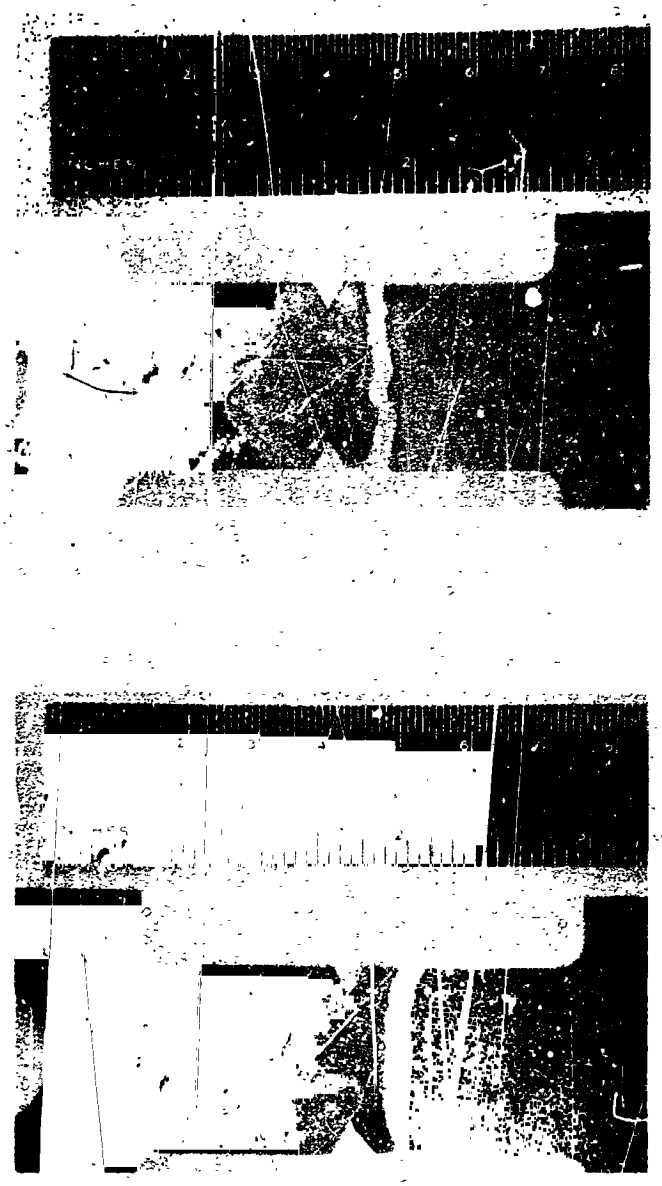

Fig. 11 LOCATION OF FAILURE AND SURFACE APPEARANCE OF EXPOSED Ti-8Al-1Mo-1V SPECIMEN. TOP TRANSVERSE, BOTTOM LONGITUDINAL.

	S.U. avg. unexp. and air exp.	MRL salt exp.		
exp. temp.	R.T. and 650°F	450°F	500°F	600°F
longitudinal	.3-.7 mil N.R. fatigue crack	○	△	♀
transverse		●	▲	♀

	NASA avg. unexp. and air exp.	MRL salt exp.			
exp. temp.	R.T. and 650°F	500°F	550°F	600°F	
longitudinal	——	○	△	♀	0.25 mil N.R.
transverse	— —	○	▲	●	

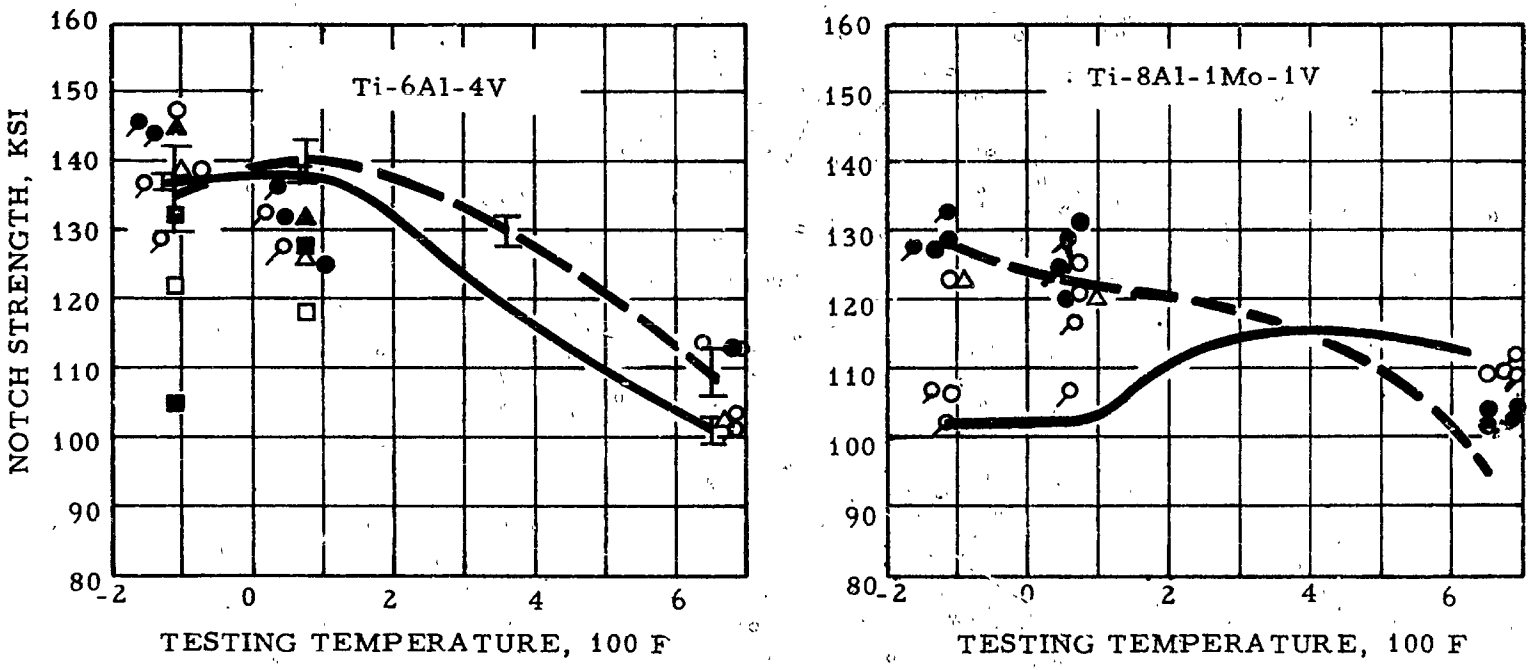

Fig. 12 EFFECT OF TESTING TEMPERATURE ON NOTCH STRENGTH OF (a) Ti-6Al-4V AND (b) Ti-8Al-1Mo-1V AFTER EXPOSURES AT VARIOUS TEMPERATURES. ALL EXPOSED SAMPLES STRESSED AT 25 KSI FOR 1000 HR AT THE INDICATED TEMPERATURES.

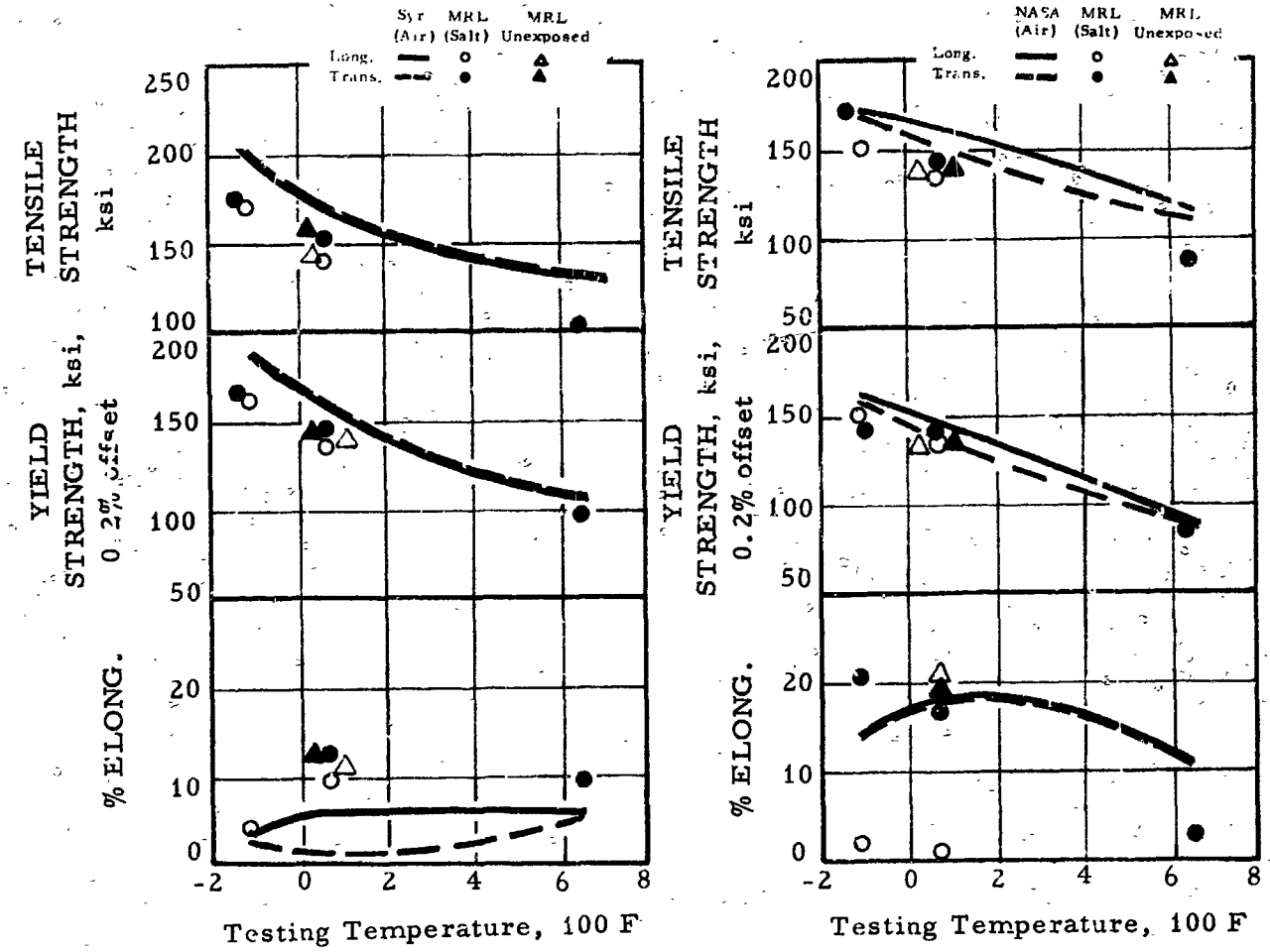

Fig. 13 COMPARISON OF TENSILE PROPERTIES RESULTING FROM AIR AND SALT EXPOSURES OF 1000 HR AND 25 ksi. Ti-6Al-4V AIR-EXPOSED DATA SUPPLIED FROM SYRACUSE UNIVERSITY; Ti-8Al-1Mo-1V AIR-EXPOSED DATA SUPPLIED FROM NASA. THE AIR EXPOSURES WERE AT 650 F WHILE THE SALT EXPOSURES WERE AT 600 F.

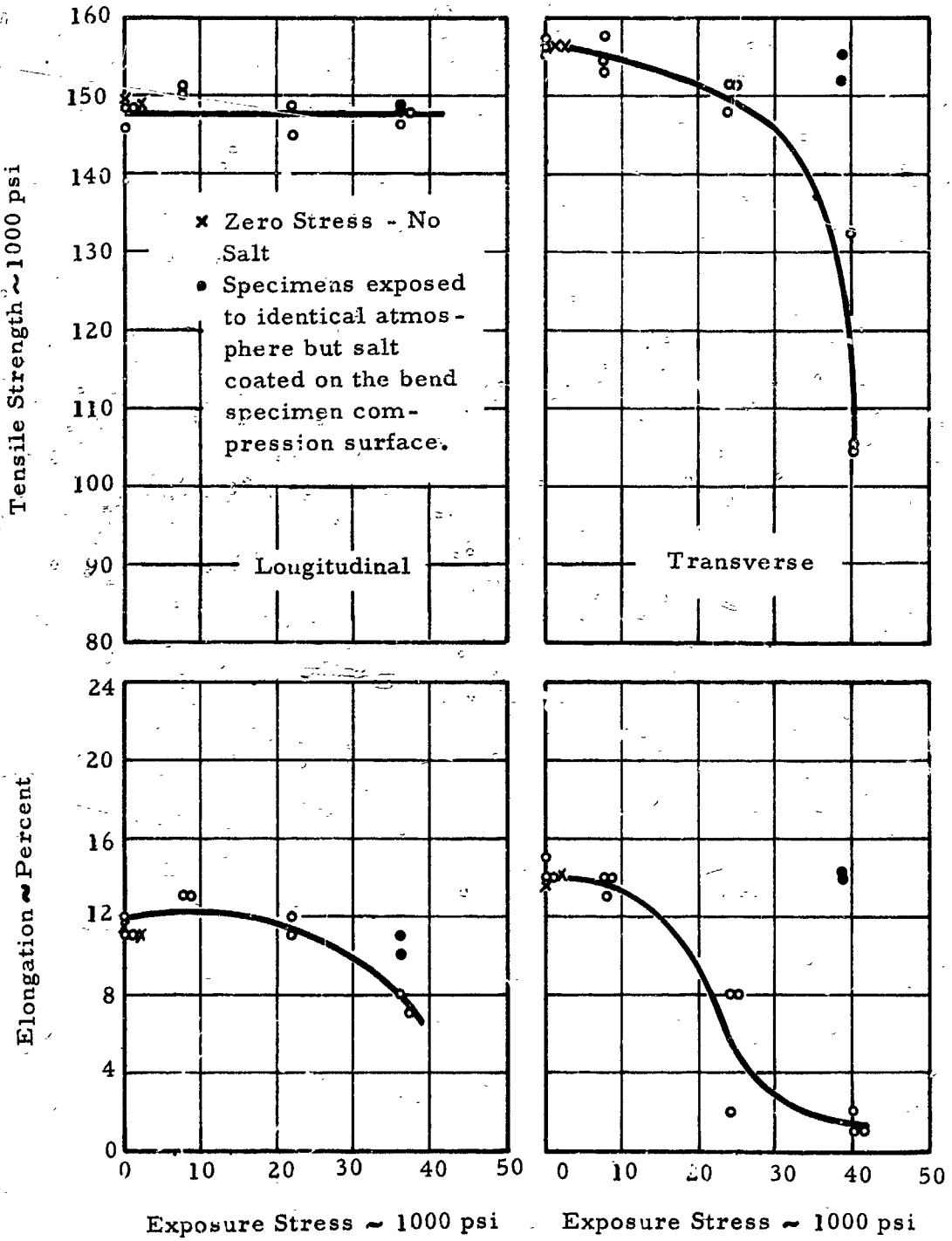

Fig. 14 EFFECT OF EXPOSURE STRESS (SURFACE STRESS IN BENDING) AT 650°F FOR 100 HOURS ON SEA SALT COATED Ti-6Al-4V (ANNEALED) TITANIUM. TESTING TEMPERATURE AT 75°F.

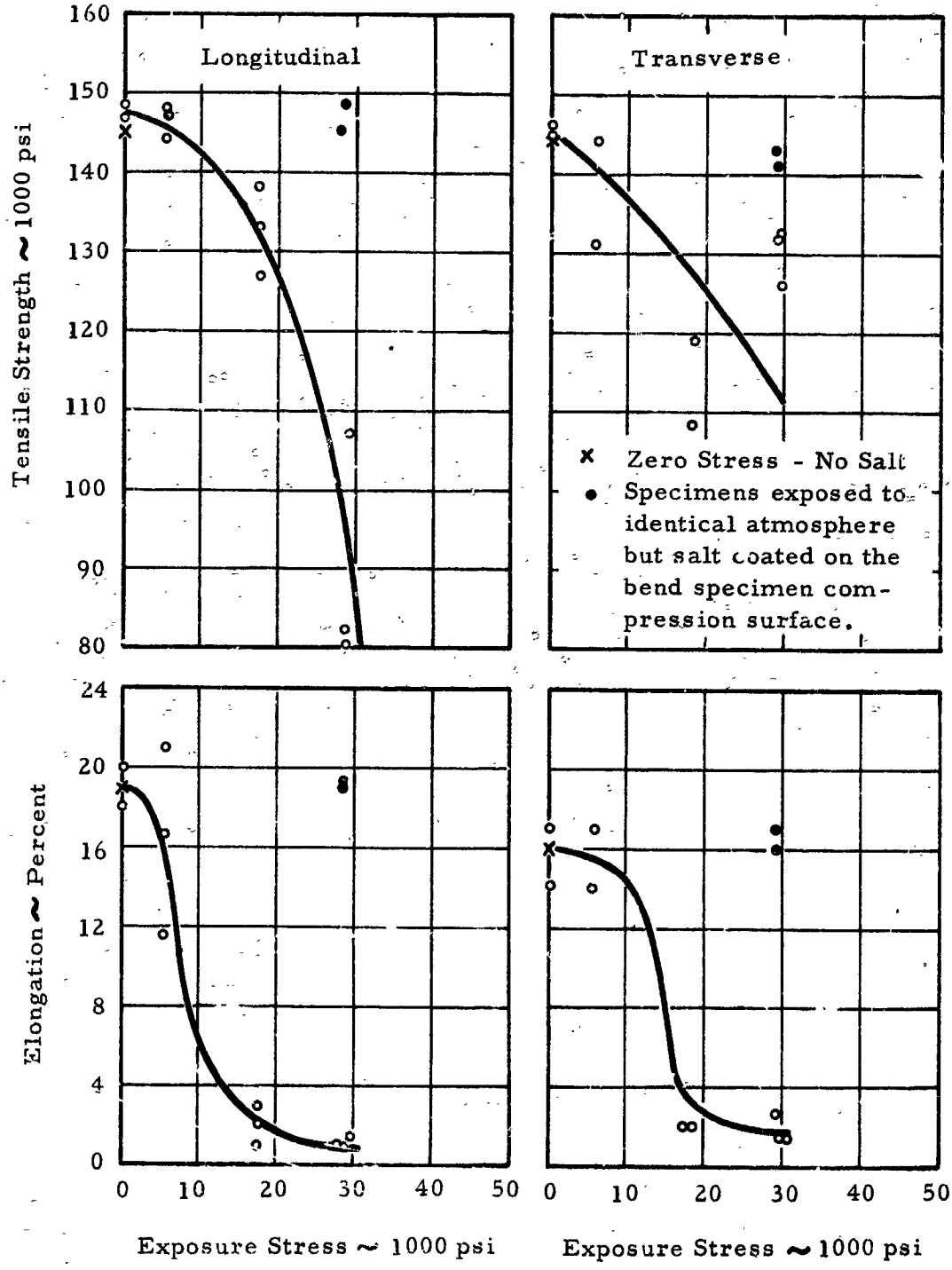

Fig. 15 EFFECT OF EXPOSURE STRESS (SURFACE STRESS IN BENDING) AT 650°F FOR 100 HOURS ON SEA SALT COATED 8Al-1Mo-1V (ANNEALED) TITANIUM. TESTING TEMPERATURE AT 75°F.

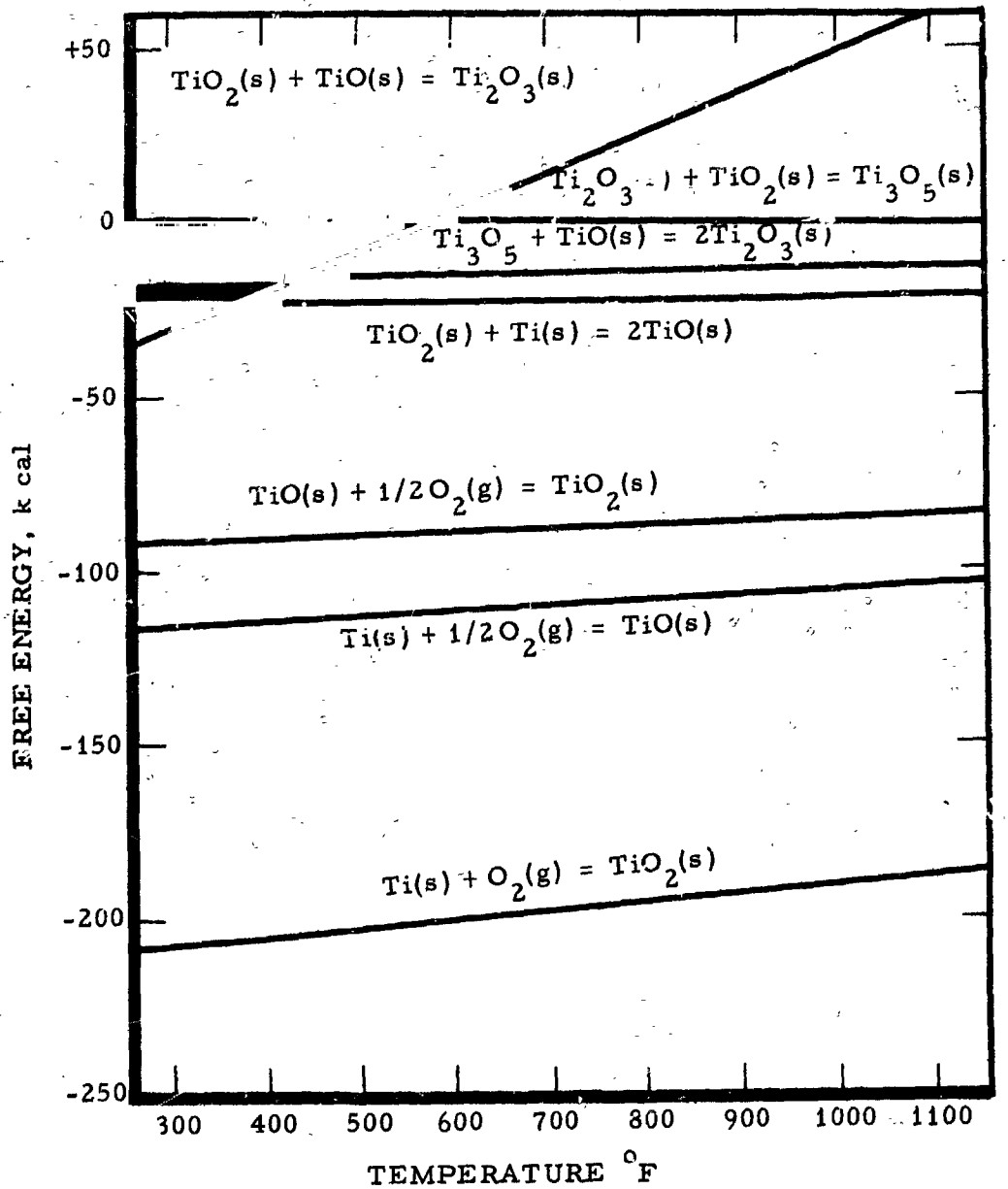

Fig. 16 FREE ENERGY AS A FUNCTION OF TEMPERATURE FOR REACTIONS OF TITANIUM AND TITANIUM OXIDES (8) (16).

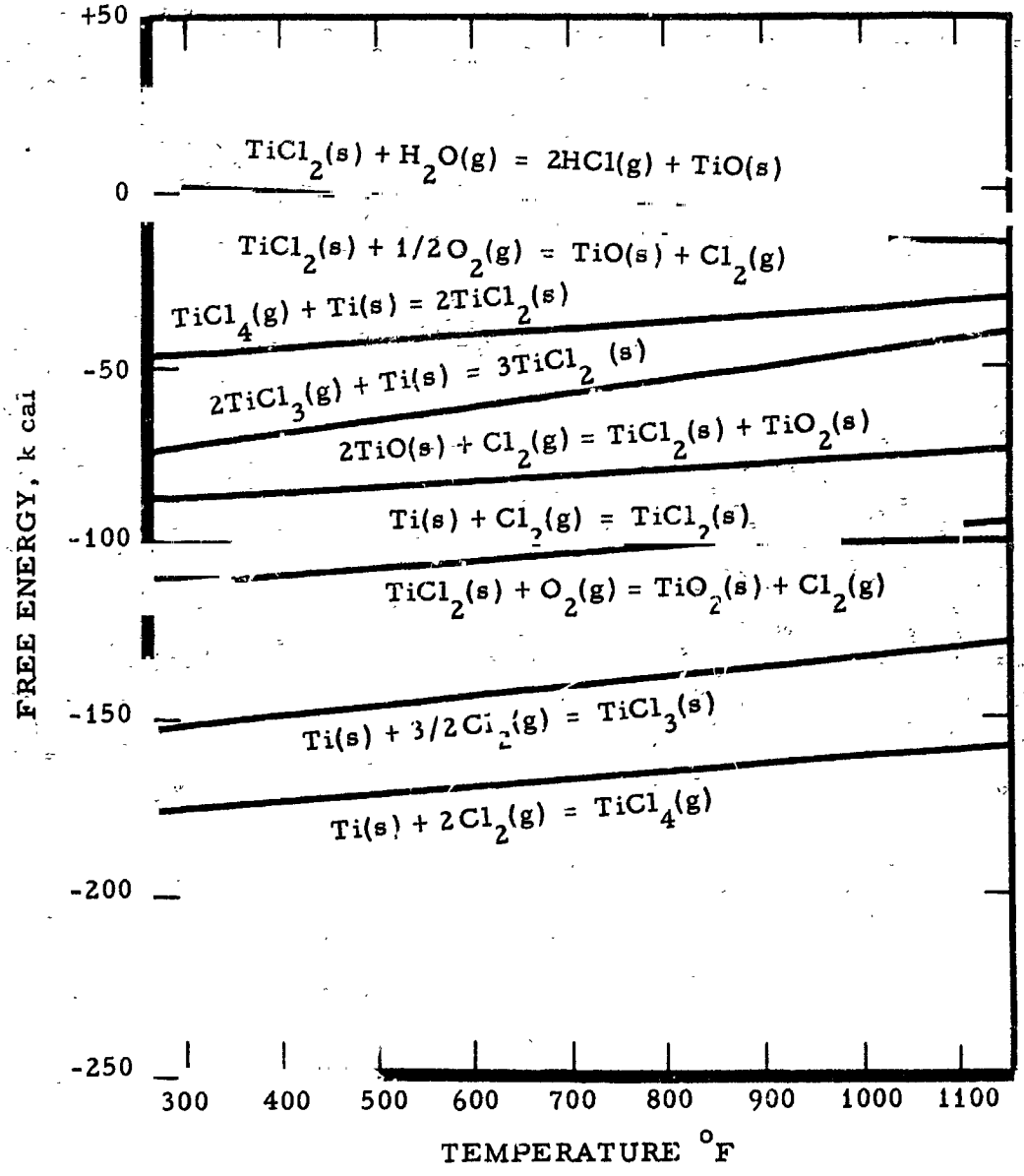

Fig. 17 FREE ENERGY AS A FUNCTION OF TEMPERATURE FOR REACTIONS OF TITANIUM CHLORIDES (8) (16).

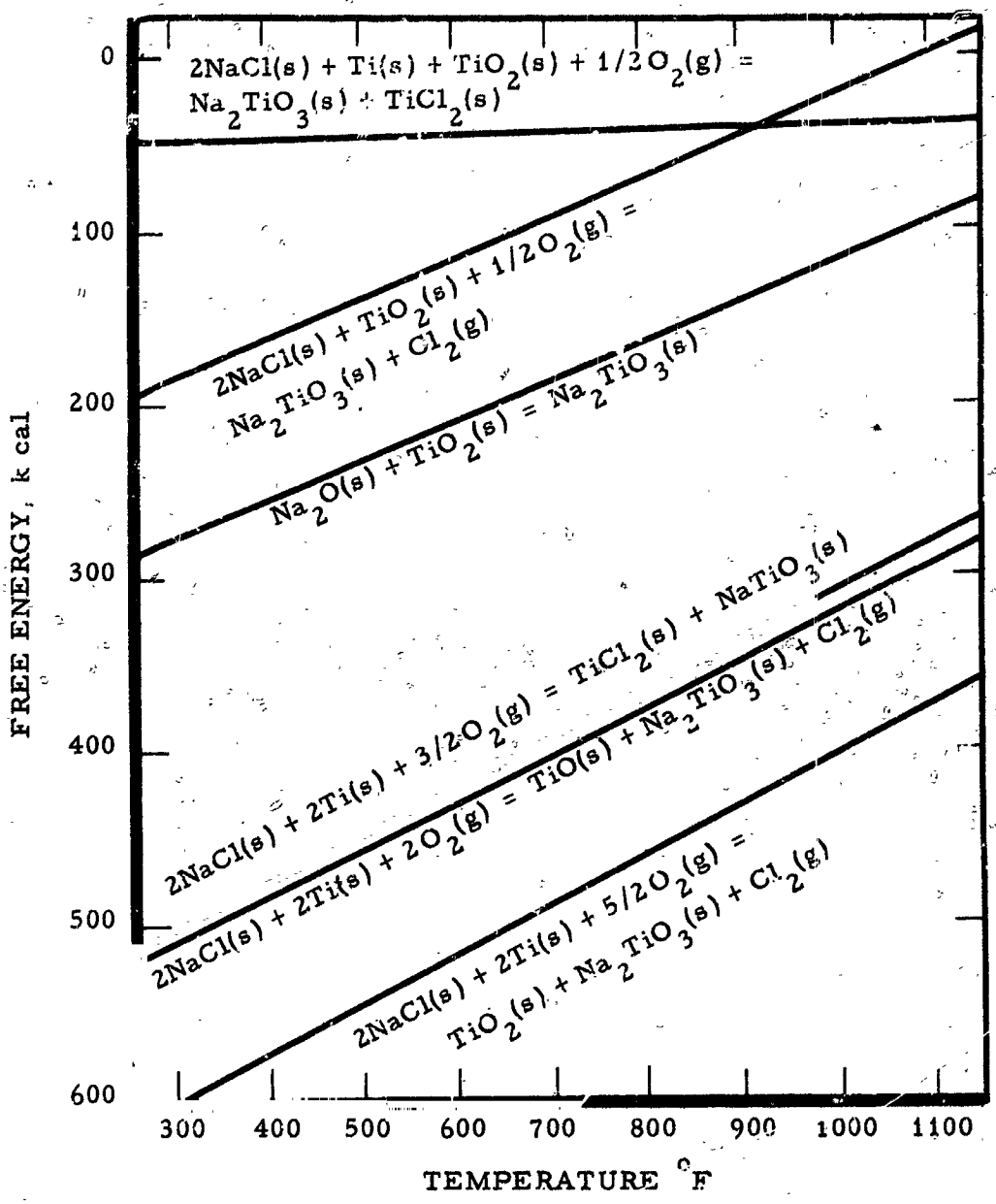

Fig. 18 FREE ENERGY AS A FUNCTION OF TEMPERATURE FOR REACTIONS OF SODIUM CHLORIDE WITH TITANIUM (8) (16).

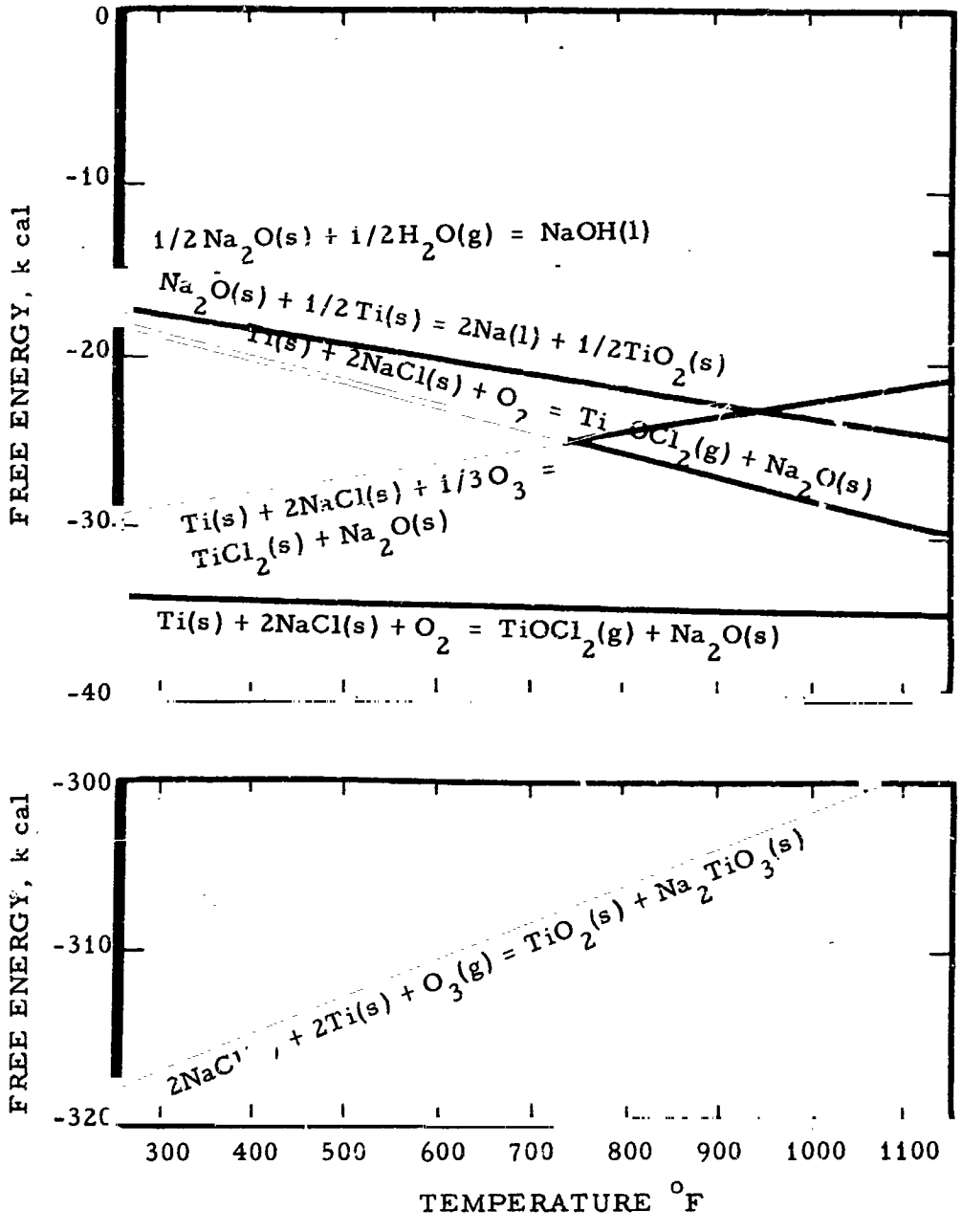

Fig. 19 FREE ENERGY AS A FUNCTION OF TEMPERATURE FOR REACTIONS OF TITANIUM, OZONE, OXIDES, AND OXYCHLORIDES (8) (16).

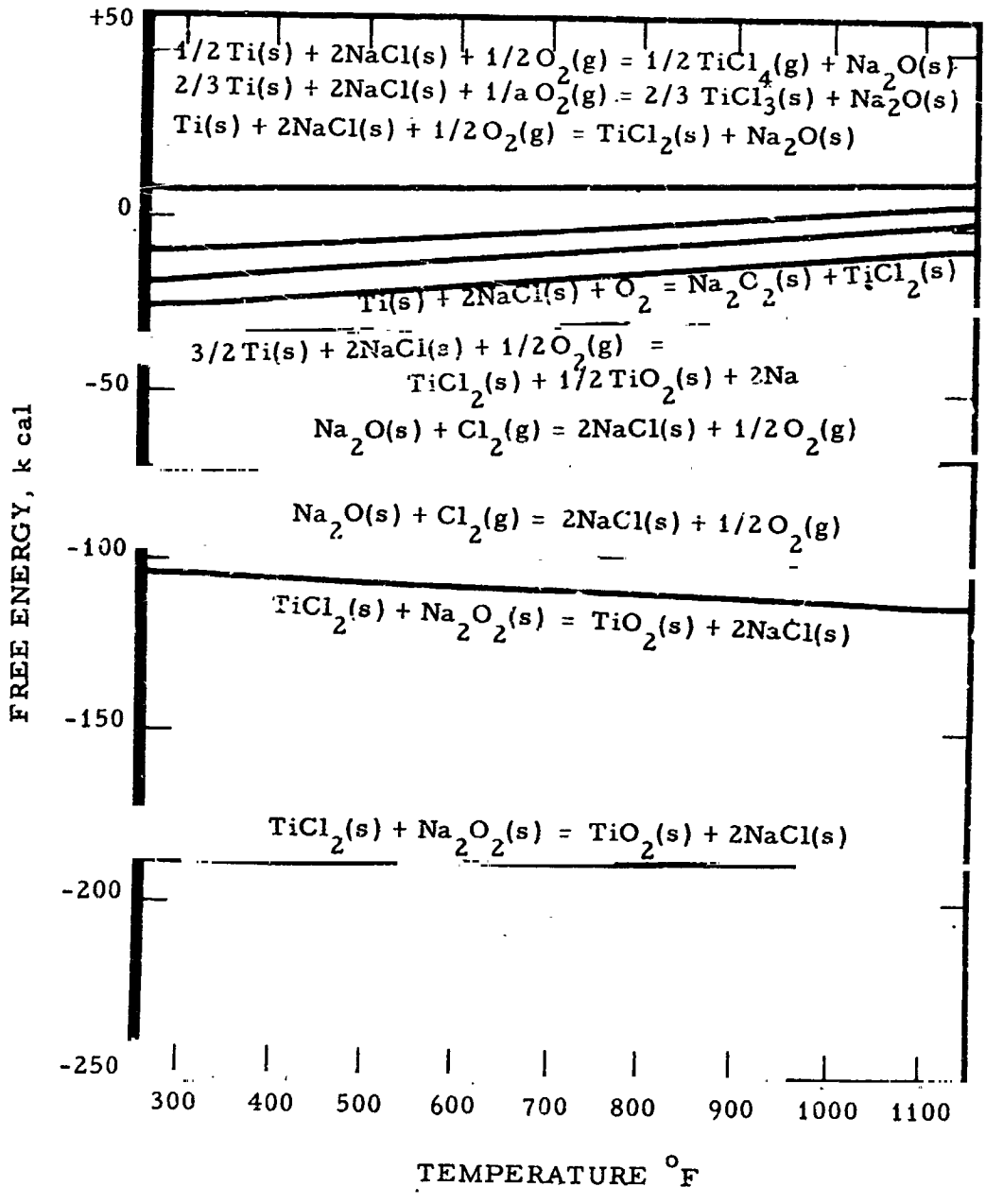

Fig. 20 FREE ENERGY AS A FUNCTION OF TEMPERATURE FOR REACTIONS OF TITANIUM CHLORIDE, OXIDES, AND SODIUM CHLORIDE (8) (16).

Fig. 21 CONDUCTIVITY CELL

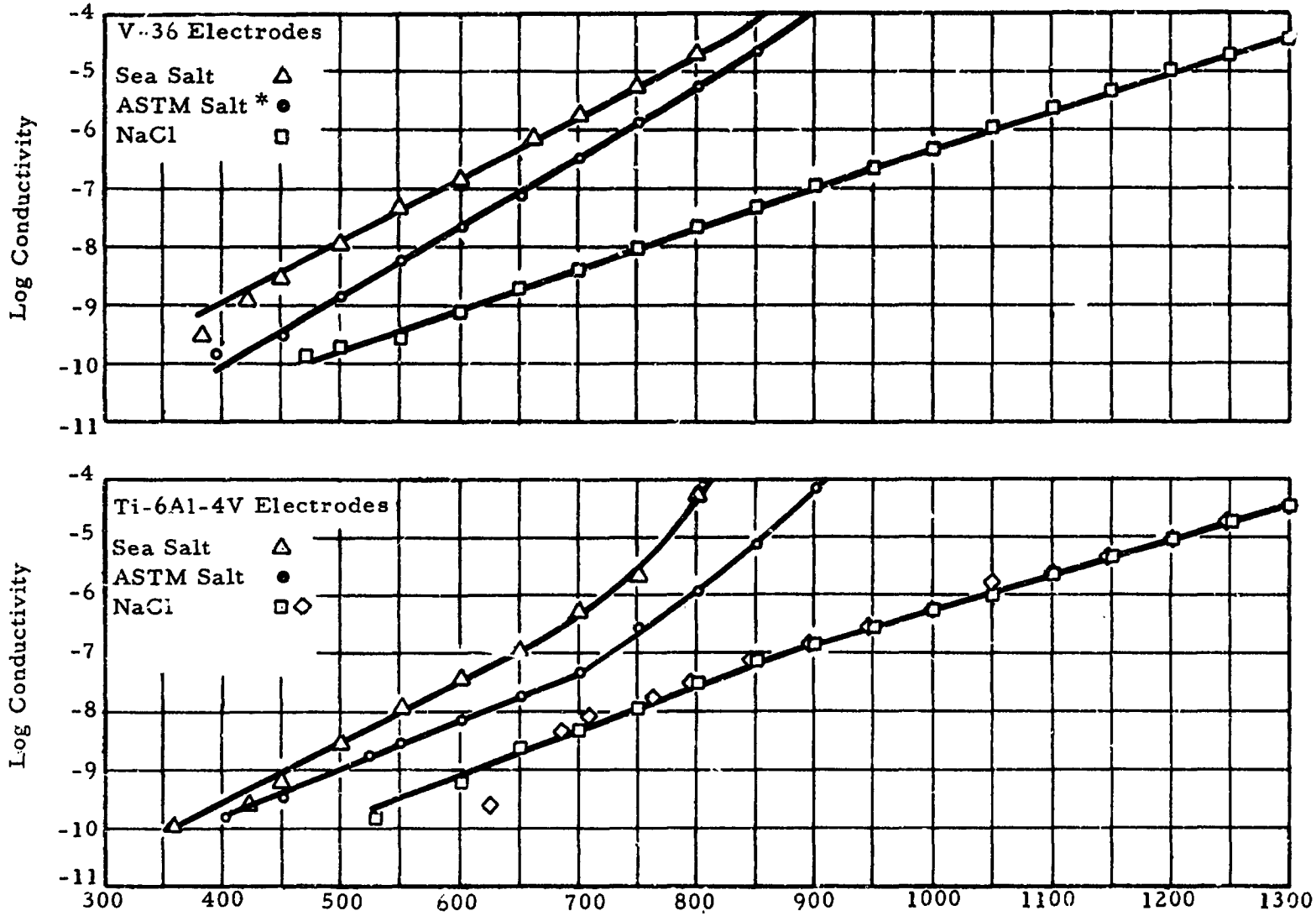

Fig. 22 LOG CONDUCTIVITY OF VARIOUS SALTS AS A FUNCTION OF TEMPERATURE.
CONDUCTIVITY CALCULATED IN $(ohm\text{-}cm)^{-1}$
* 7 PARTS NaCl TO 1 PART $MgCl_2$

Fig. 23 TITANIUM TEST SPECIMEN COATED WITH SALT AND TITANIUM ELECTRODES.

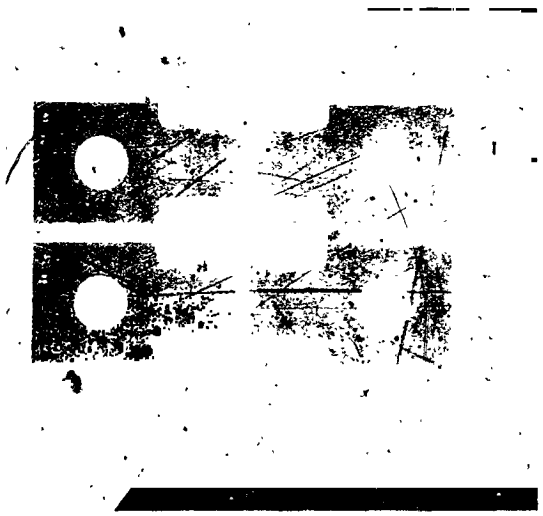

Fig. 24 FRACTURED Ti-6Al-4V NOTCH SAMPLES AFTER 650°F EXPOSURE TO SEA SALT AND AN EXTERNALLY APPLIED CURRENT.

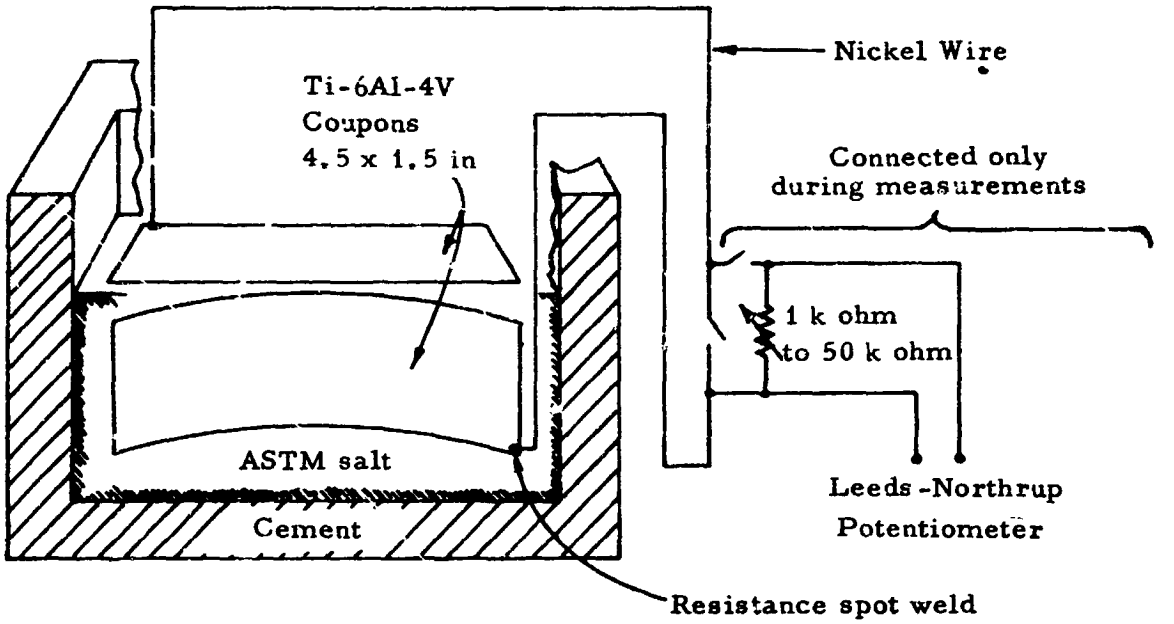

Fig. 25 FORMATION OF AN ELECTROLYTIC CELL BY DIFFERENTIAL AERATION OF Ti-6Al-4V COUPONS.

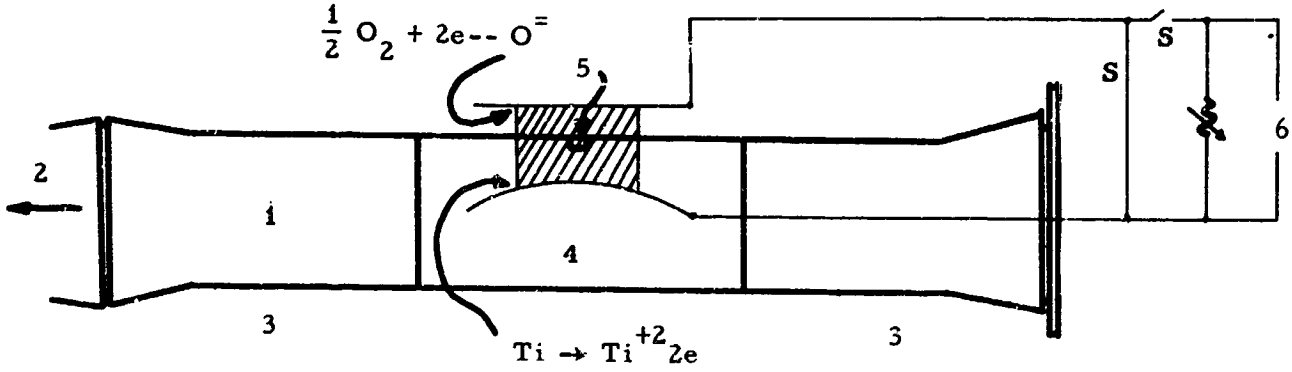

Fig. 26 SCHEMATIC DIAGRAM OF CONTROLLED ATMOSPHERE CORROSION CELL.

1. Vacuum tube
2. To cold trap
3. Glass ends of 4 inch diameter tube
4. Glazed alundum tube sealed to glass (glazed to prevent porosity)
5. Unglazed area on tube permeated with salt
6. Potentiometer

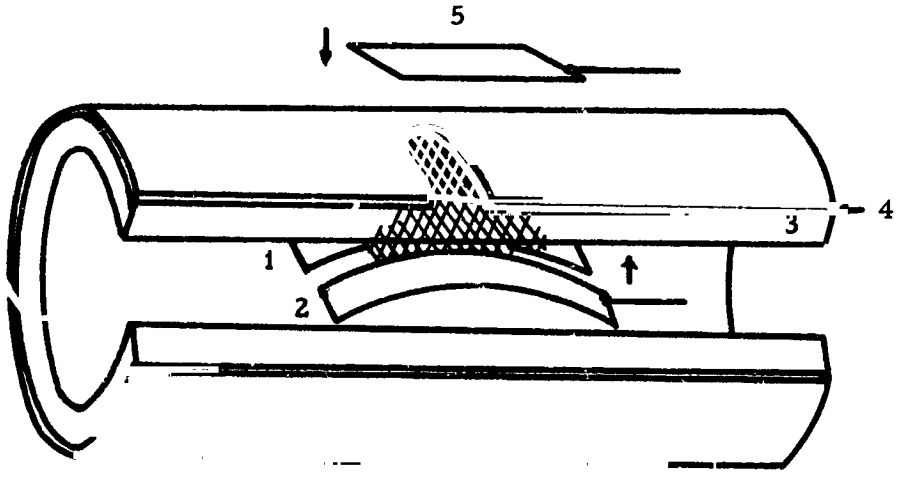

Fig. 27 PLACEMENT OF COUPLED AND UNCOUPLED BEND SAMPLES IN POROUS SECTION OF CONTROLLED ATMOSPHERE CORROSION CELL.

1. Control Sample
2. Coupled sample (anode)
3. Four-inch alundum tube
4. Glaze
5. Air exposed sample (cathode)

a. Vacuum read-out system
b. Ionization gage
c. Thermocouple gages
d. Cold trap
e. Leeds-Northrup mv recorder set up for measuring corrosion currents
f. High impedence volt meter
g. Furnace
h. Corrosion cell
i. Mechanical pump
j. Diffusion pump

Fig. 28 PHOTOGRAPH OF CONTROLLED ATMOSPHERE APPARATUS

(a)

(b)

Fig 29 CONDITION OF BEND SAMPLES AFTER REMOVAL FROM CORROSION CELL. CONTROL SAMPLE IS IN REAR, COUPLED SAMPLE IS IN FOREGROUND.
(a) TOP VIEW, (b) OBLIQUE VIEW.

Fig. 30 STRESS CORROSION CRACK AT LIQUID SALT EDGE. SAMPLE WAS STRESS TO 80 KSI BY BENDING. FAILURE OCCURRED AFTER 28 MINUTES AT 690°F AND $pp O_2 = 1 \times 10^{-5}$ mm Hg.

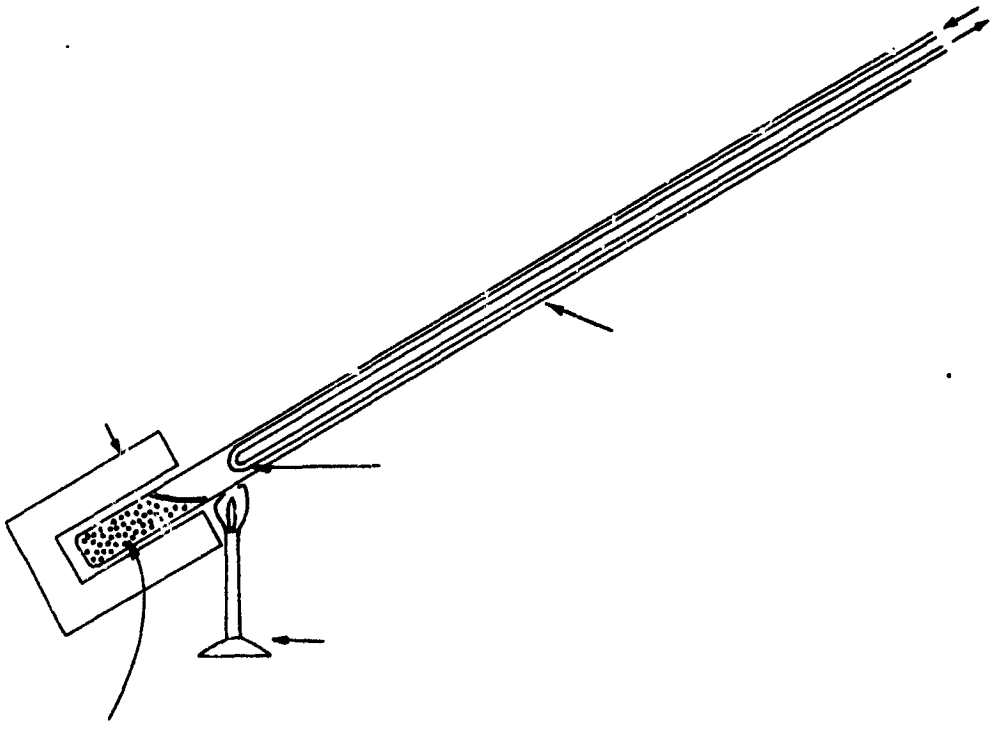

Fig. 31 DIAGRAM OF APPARATUS USED FOR COLLECTING VOLATILE PRIMARY CORROSION PRODUCTS.

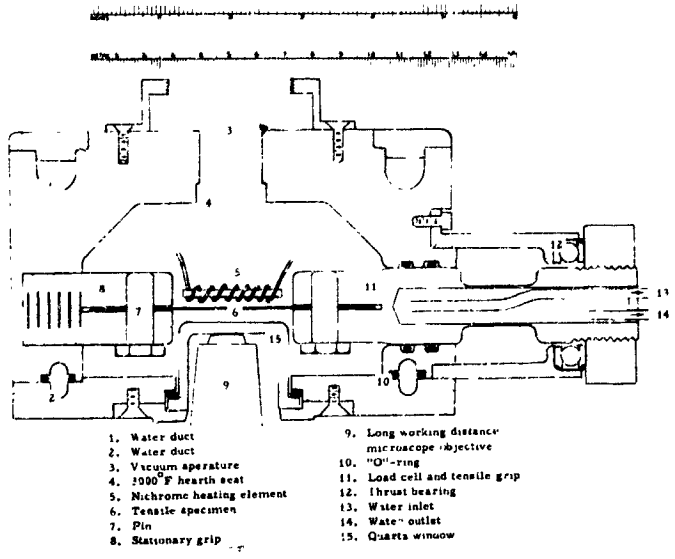

(a)

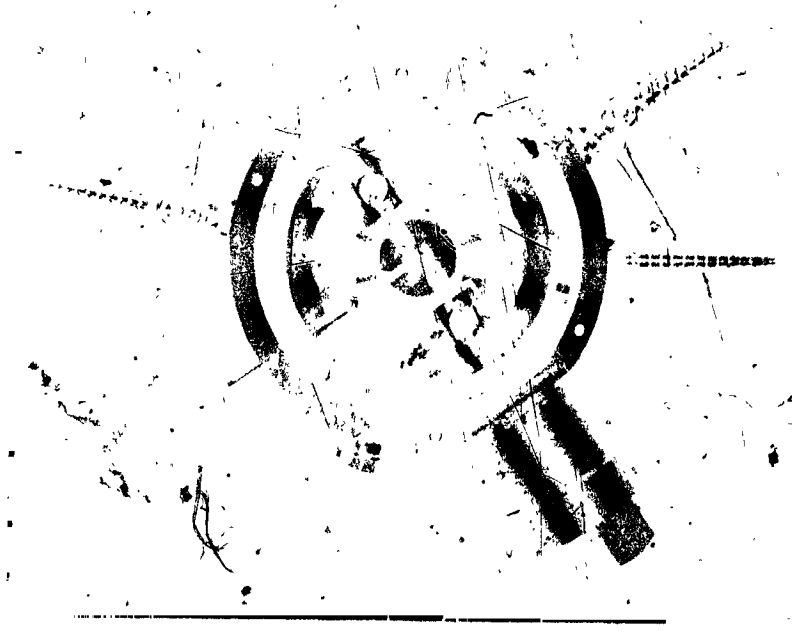

(b)

Fig. 32 a - SCHEMATIC DRAWING OF TENSILE HOT STAGE - Side View
b - PHOTOGRAPH OF INTERIOR OF HOT STAGE - Top View

Scale $\frac{2}{1}$

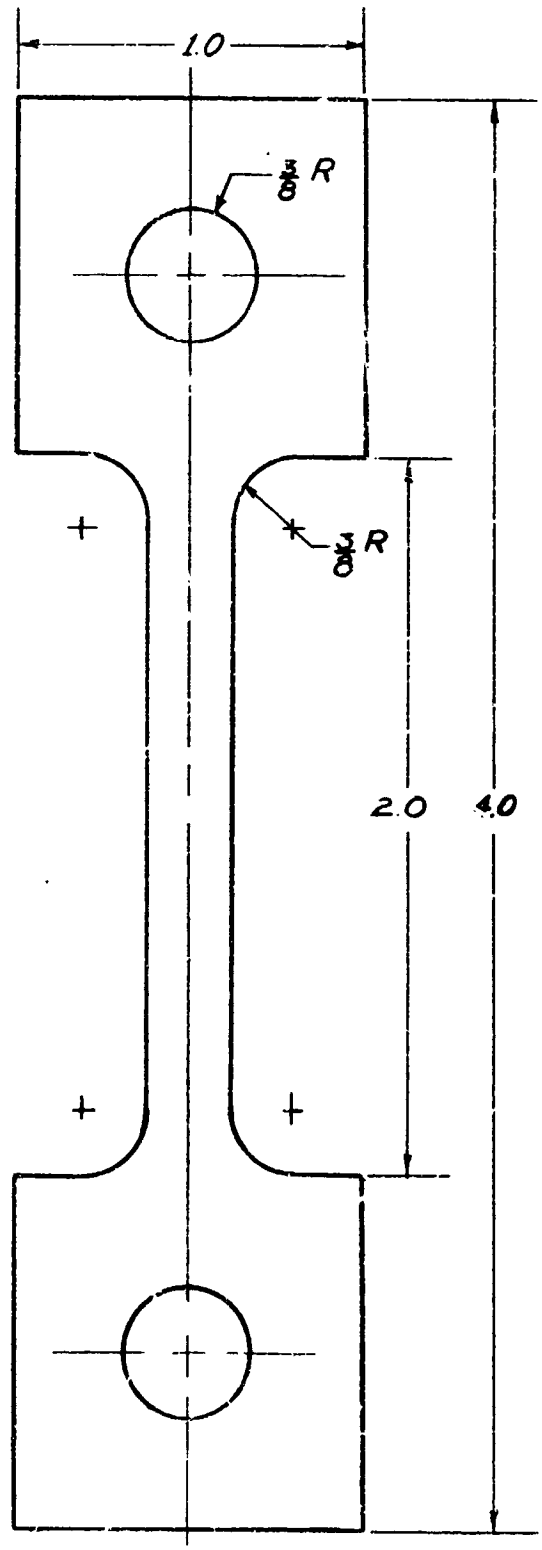

Fig. 33 DIMENSIONS OF SMOOTH HOT STAGE TEST SAMPLE

(a)

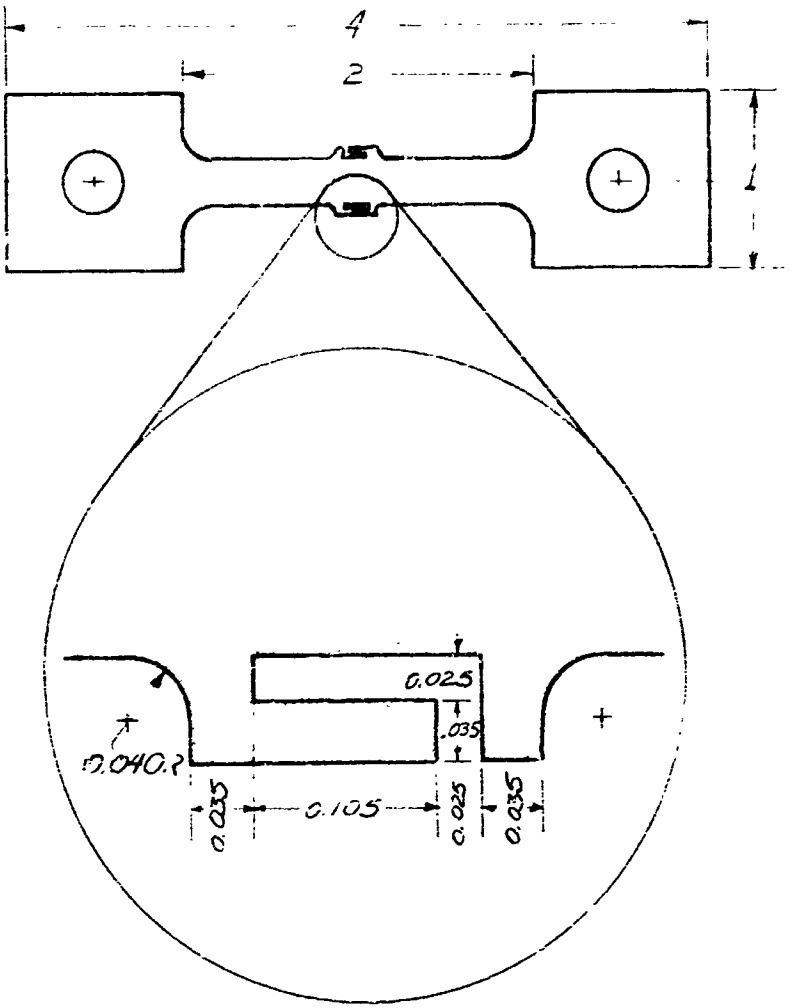

(b)

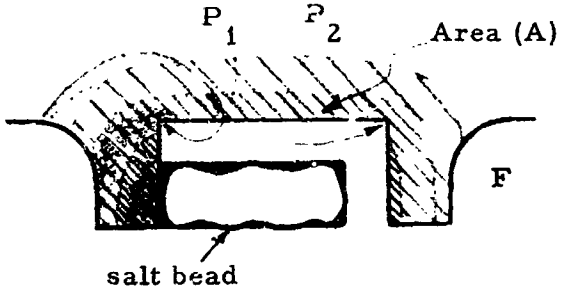

Fig. 34 a - DIMENSION OF TENSILE SAMPLE WITH SIDE HOOKS

b - LOCATION OF POINTS WHERE SOLID, LIQUID AND GASEOUS REACTION PRODUCTS FORM. CROSS HATCHED AREAS INDICATE GASEOUS CONCENTRATION AND SHADED AREAS REPRESENT SURFACE DIFFUSION PRODUCT CONCENTRATION

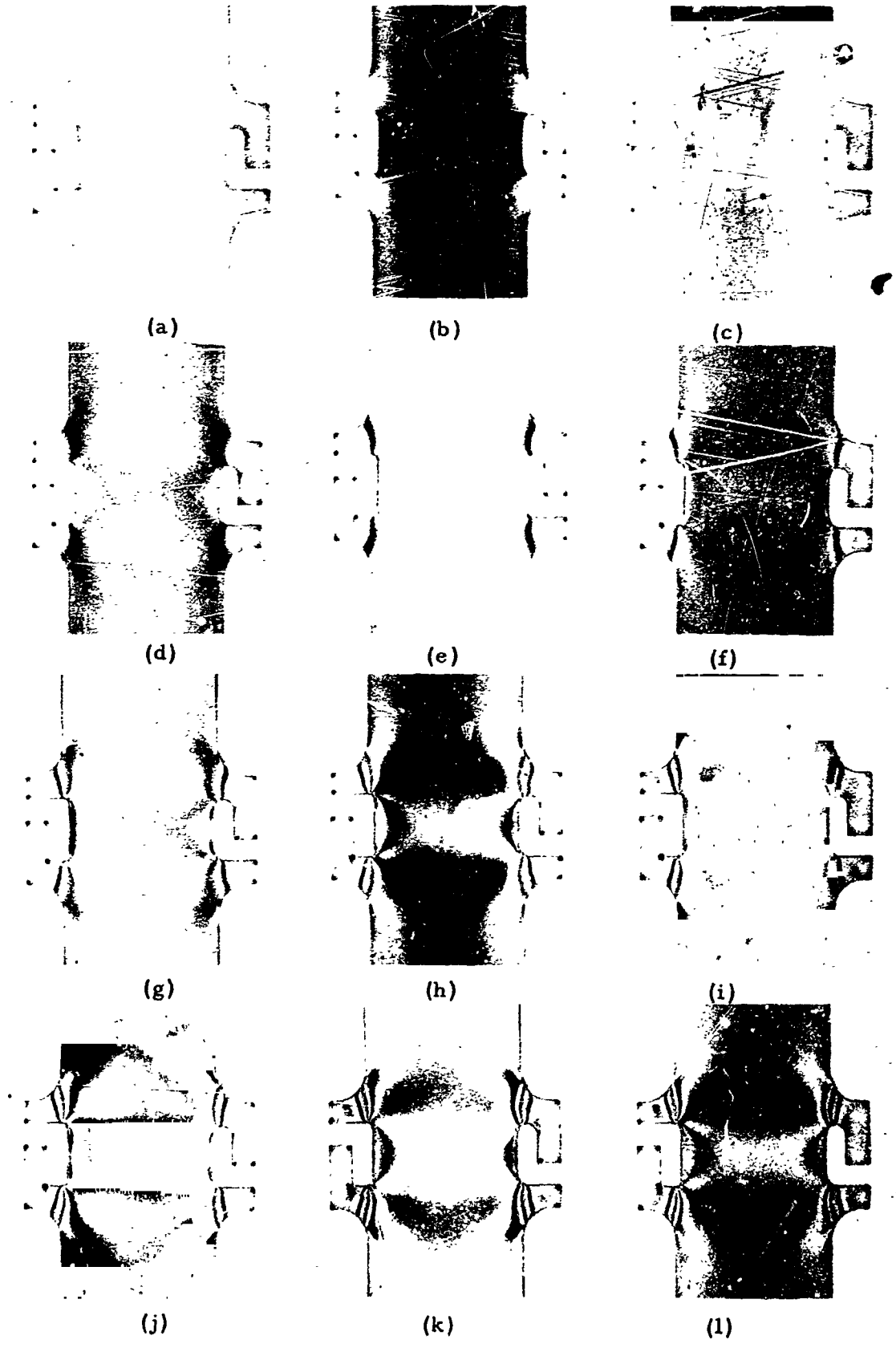

Fig. 35 STRESS PATTERN GROWTH ON PRONGED HOT STAGE SAMPLES. (a) INDICATES NO LOAD WHILE INCREASING LOADS ARE REPRESENTED BY (b) THROUGH (l). Magnification 2.2X.

Fig. 36 SMOOTH TENSILE SAMPLE OF Ti-6Al-4V, AT 650F AND 80 KSI, FOR 3 HOURS. CRACKS INITIATED FROM PERIPHERY OF SALT. SAMPLE WAS ETCHED BEFORE APPLYING A SEA SALT SLURRY. 25X.

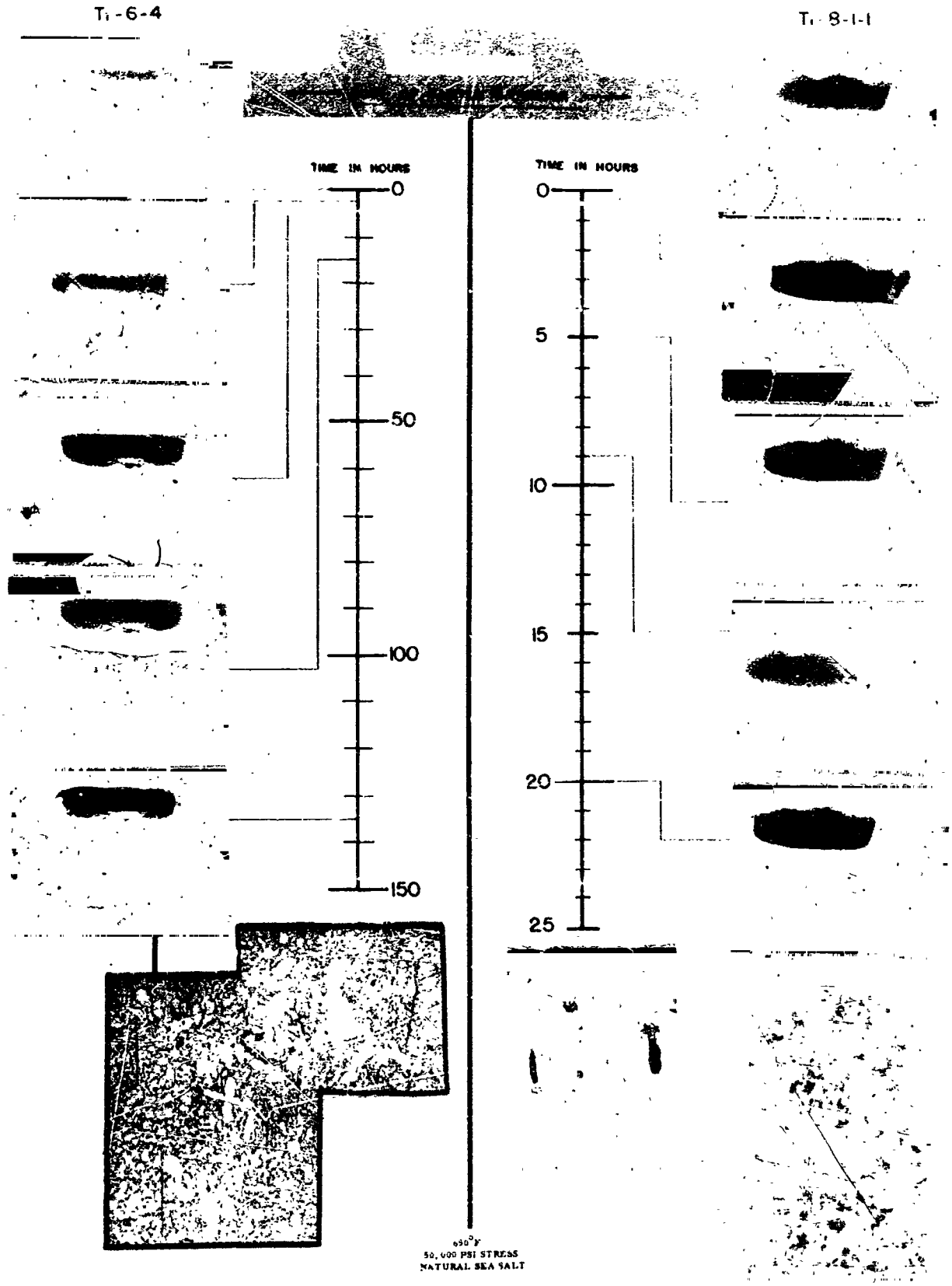

Fig. 37 TIME LAPSE STUDY OF STRESS CORROSION CRACK GROWTH IN (left) Ti-6Al-4V AND (right) Ti-8Al-1Mo-1V. MACRO PHOTOS ≈10X and Micro PHOTOS ≈ 100X.

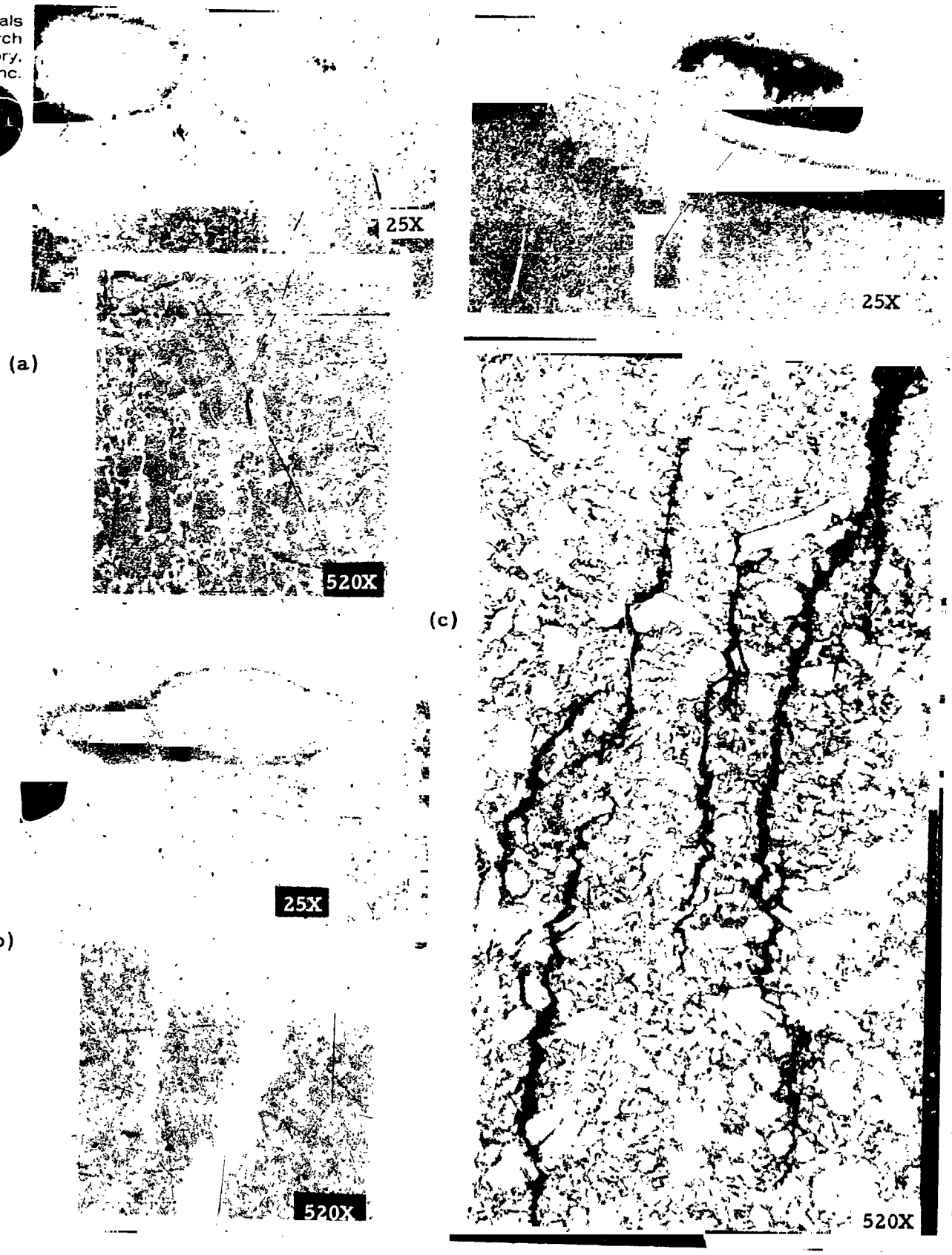

Fig. 38 STRESS CORROSION CRACKS IN Ti-6Al-4V. EXPOSED AT 650°F, 80 KSI FOR (a) 200 HR, (b) 200 HR, AND (c) 100 HR.

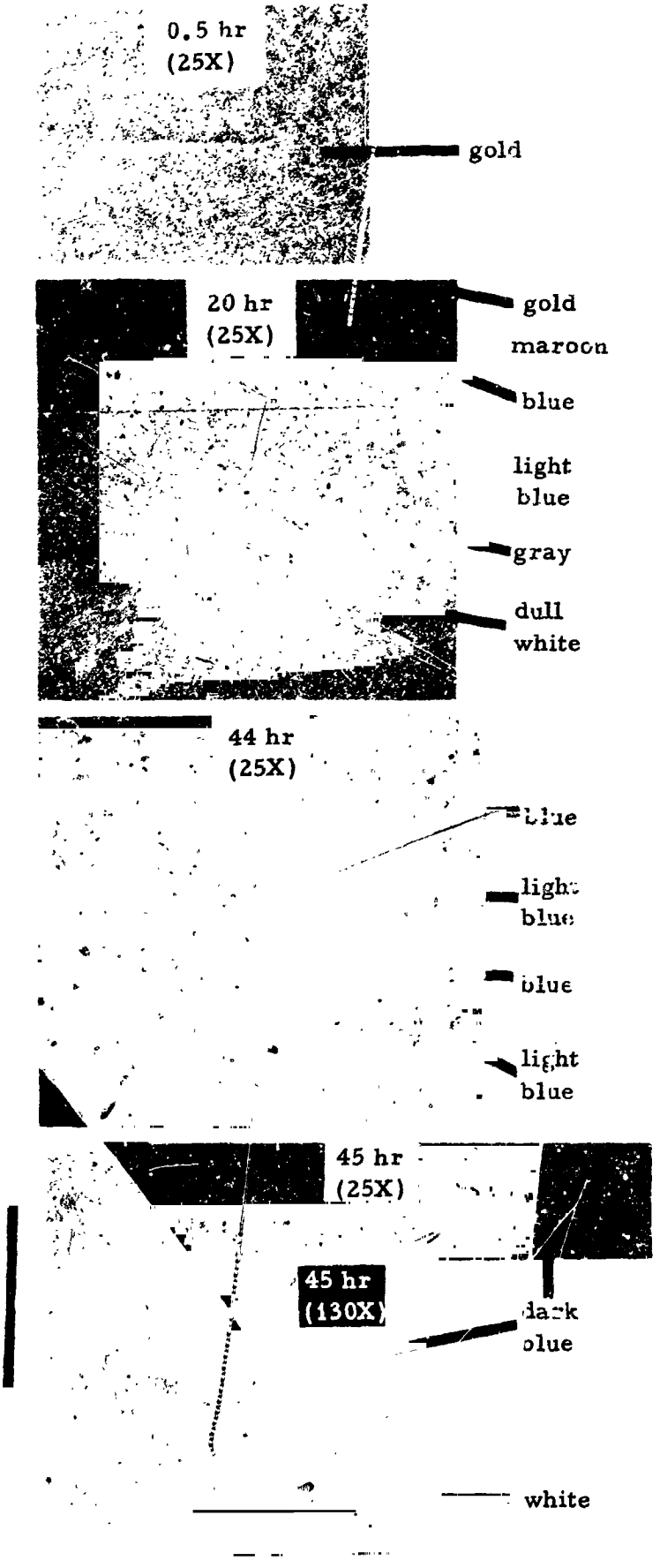

First indication of cracking. No color variation present and no indication of corrosion products. Temp maintained at 650F, stress 60 ksi. The salt is on the opposite side of the sample.

Waves of corrosion product emanating concentrically from crack in elliptical pattern. Stress dropped to 52 ksi; temp still 650F. The crack was apparently empty.

The temperature was just increased from 650F to 875F. Corrosion product began to develop measurably faster. The load was reduced to about 4 ksi. The crack began to fill with a crust of corrosion product.

Temperature raised to 1120F for 15 minutes, then lowered to R.T. A liquid was seen at this temperature and the evidence of it is shown in these photographs taken at R.T. The liquid has migrated, by capillary action, to the most narrow regions of the crack, and has oozed out at the crack tip.

Fig. 39 DEVELOPMENT OF CRACK AND CORROSION PRODUCTS IN Ti-6Al-4V.

(a) Side view
62X

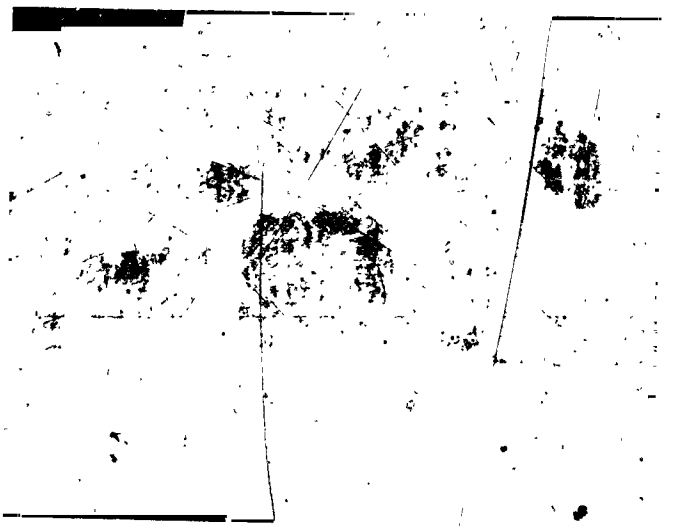

(b) Top view
25X

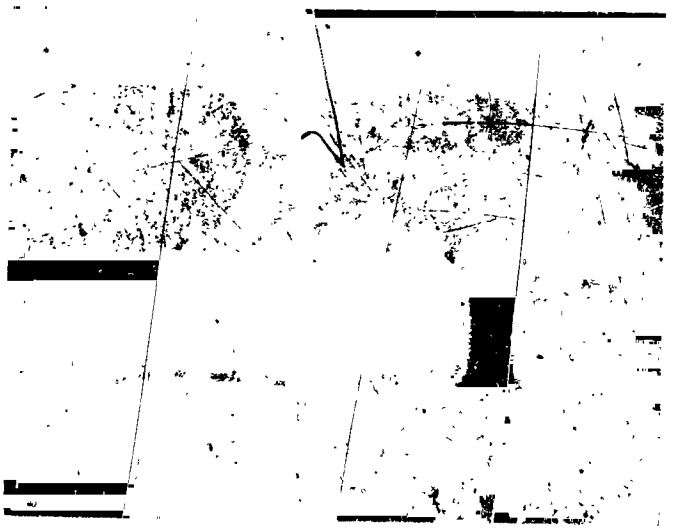

Fig. 40 PHOTOGRAPHS SHOWING CORRODED AREA OF A Ti-6Al-4V PRONGED SAMPLE AFTER EXPOSURE TO SEA SALT AT 650°F FOR 200 HR.

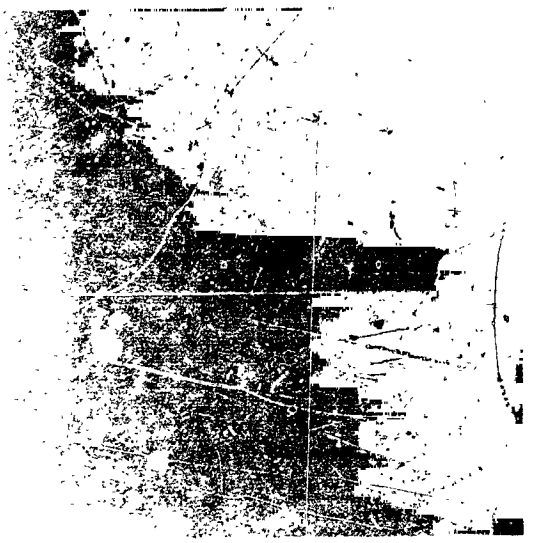

Neg. No. MP 657 X1500

Fig. 1

Electron Image

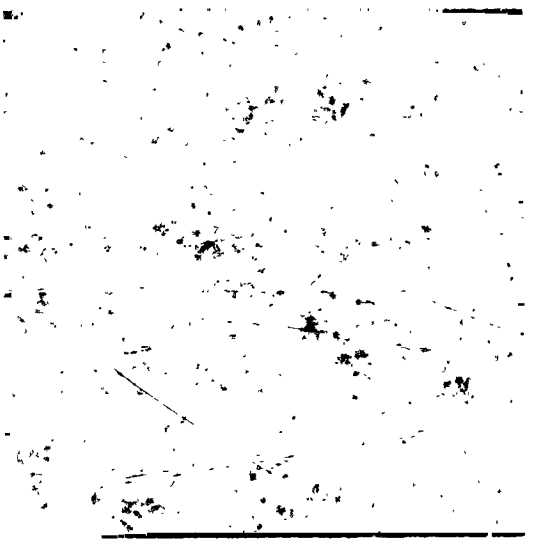

Neg. No. MP 650 X1500

Fig. 2

Mo Lα X-ray Image

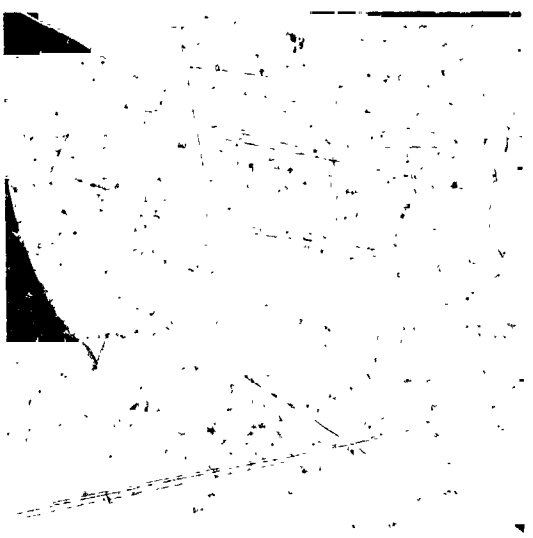

Neg. No. MP 658 X1500

Fig. 3

Al Kα X-ray Image

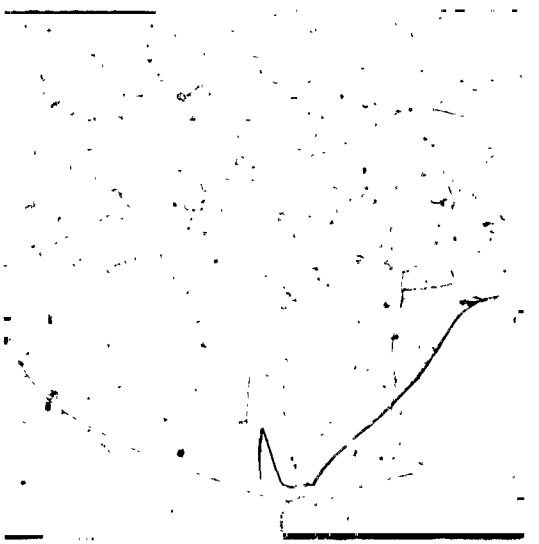

Neg. No. MP 659 X1500

Fig. 4

V Kβ X-ray Image

Fig. 41 ELECTRON PROBE STUDY OF ALLOY SEGREGATION IN Ti-8Al-1Mo-1V.

REFERENCES

1. Raring, R. H., Materials Research and Standards, Vol. 13, No. 10, October, 1963.

2. Supersonic Transports, a report by the Supersonic Transport Group, Bureau of Flight Standards, F.A.A., Washington, D.C., March, 1961.

3. Symposium on Supersonic Air Transports, Vol. 1, 14th Technical Conference, National Air Transport Association, Montreal 3, Canada, April, 1961.

4. Progress Report on the Salt Corrosion of Titanium Alloys at Elevated Temperature and Stress, Battelle Memorial Institute, TML Report 88, November, 1957.

5. Sell, R. J., Chave, C., and Weiss, V., Material Evaluation for Mach III Transport Plane, Quarterly Progress Report #3, Syracuse University, February, 1962.

6. Espey, G. B., Bubsey, R. T., and Brown, W. F., Jr., A Preliminary Report on the NASA Sheet Alloy Screening Program for Mach 3 Transport Skins, Proc. ASTM, Vol. 62, 1962.

7. Covington, L. C. and Beck, K. O., Studies of Mechanisms of Stress Corrosion, TMCA Project 47-42 Progress Report No. 1, June, 1957.

8. Kochka, E. L., and Petersen, V. C., The Salt Corrosion of Titanium Alloys at Elevated Temperatures, Final Technical Report, Crucible Steel Company, January, 1961.

9. Special Committee on Material Research for Supersonic Transports, Minutes of the 10th Meeting NASA, Washington 25, D.C., February, 1964.

10. Kirchner, R. L., and Ripling, E. J., Elevated Temperature Stress Corrosion of High Strength Sheet Materials in the Presence of Stress Concentrators, Materials Research Laboratory, Inc., Richton Park, Illinois, May, 1964.

11. Straumanis, M. E., and Chen, P. C., The Corrosion of Titanium in Acids, Corrosion, Vol. 7, 1951.

12. Schlechter, A. W., Straumanis, M. E., and Gill, C. B., Deposition of Titanium Coatings from Pyrosols, Journal of the Electrochemical Society, Vol. 102, No. 2, February, 1955.

13. Straumanis, M. E., and Schlechter, A. W., Electrochemical Behavior of A Titanium-Fused Salt-Platinum Cell, Journal of the Electrochemical Society, Vol. 102, No. 3, March, 1955.

14. Shis, S. T., Straumanis, M. E., and Schlechter, A. W., Deposition of Titanium from Titanium-Oxygen Alloys on Copper, Iron, and Mild Steel, Journal of the Electrochemical Society, Vol. 103, No. 7, July, 1956.

15. Crossley, F. A., Reichel, C. J., and Simcoe, C. R., The Determination of the Effects of Elevated Temperatures on the Stress Corrosion Behavior of Structural Materials, Armour Research Foundation, WADC TR 60-191, May, 1960.

16. Notes on Hot Salt Cracking of Titanium, Battele Memorial Institute, January, 1964.

17. Braski, D. N., and Heimerl, C. J., The Relative Susceptibility of Four Commercial Titanium Alloys to Salt Stress Corrosion at 550°F, NASA, TND-2011, July, 1963.

18. Avery, C. H., and Turley, R. V., Screening Test Program for Evaluation of the Stress Corrosion Susceptibility of Alloys Under Consideration for Application as Skin Materials, Douglas Aircraft Company, Inc., Report No. 31421, April, 1963.

19. Straumanis, M. E., private communication.

20. Kirchner, R. L., and Ripling. E. J., Elevated Temperature Stress Corrosion of High Strength Sheet Materials in the Presence of Stress Concentrators, Materials Research Laboratory, Inc., Richton Park, Illinois, August, 1962.

21. Kormorek, K., and Herasymenko, P., Equilibria Between Titanium Metal and Solutions of Titanium Dichloride in Fused Sodium Chloride, Journal Electrochemical Society, Vol. 105, 1958.

22. Martin, George, Stress Corrosion Effects at Elevated Temperature of Some Aircraft Materials, National Association of Corrosion Engineers 20th Annual Conference, Chicago, Illinois, March, 1964.

23. Dreyer, G. A., Investigation of Susceptibility of High Strength Martensitic Steel Alloys to Stress Corrosion, The Boeing Company Transport Division, Renton, Washington, Technical Report No. ASD-TDR-62-876, September, 1962.

APPENDIX A

A CHRONOLOGICAL REVIEW OF PUBLICATIONS PERTINENT TO THE MECHANISM OF HOT DRY SALT STRESS CORROSION CRACKING OF TITANIUM.

Titanium Metals Corporation of America (7)

The first work done in this area was by Titanium Metals Corporation of America Their results were compiled in an unpublished progress report, "Stress Corrosion", June 1957.

Corrosion Rates - Differences in corrosion rates among commercially pure titanium and various titanium alloys have been found to be small. Titanium alloys, Ti-5Cr, Ti-5Ni, Ti-3Al, Ti-5Al, Ti-6Al, Ti-3Zr, Ti-6Al-4V-.5Fe (90BHN sponge), Ti-6Al-4V-.5Fe, Ti-6Al-4V-1Fe, Ti-6Al-4V-2Fe, Ti-75A, Ti-5V, Ti-.25Fe, and Ti-1Fe were exposed to air and sodium chloride at elevated temperatures. Only small differences could be observed in the amount of attack.

Role of oxygen - In the absence of other oxidizing agents, oxygen must be present for corrosion to occur. Unstressed samples were placed in contact with sodium chloride for 24 hr at 1300°F in vacuum and also in purified argon with no resulting attack. A test run in unpurified argon resulted in the development of an oxide scale in those areas not covered by salt. Pure oxygen did not increase the corrosion rate much over that caused by air tests in sodium chloride.

Importance of physical contact - Physical contact between the titanium and solid sodium chloride is required for corrosion to take place. Titanium samples were suspended 1/4 in. above a bed of dry NaCl. No corrosion pits developed in 24 hr at 1100°F or in 72 hr at 1300°F, although a yellow scale did develop at the higher temperature.

Effect of water vapor - Water vapor within the limits studied has no effect on general corrosion rate. Titanium samples coated with NaCl were exposed to an oxygen atmosphere that was

(1) dry, (2) saturated with water vapor, and (3) saturated with hydrogen chloride. In the latter two cases, oxygen was bubbled through water and concentrated HCl respectively. No differences in the corrosion rates were observed in the three situations. These samples, however, were not under stress at the time of exposure, and the exposure temperature is unknown.

Effect of acidic oxides - In tests run in hot air furnaces, sodium chloride individually mixed with the acidic oxides Al_2O_3, Cb_2O_5, CrO_3, Fe_2O_3, MnO_2, Sb_2O_3, SnO, TiO_2, ground pyrex glass, ground quartz glass and ground Coors porcelain crucible were found to increase general corrosion rates tremendously, while V_2O_5 and P_2O_5 increased the rate only slightly. The basic oxides BaO, and CuO, and ZrO_2 as well as the substances Na_2SO_4, Na_2CO_3, graphite, and silicon carbide, did not increase the corrosion rate.

Reaction products and suggested reactions - Chlorine and titanium dichloride may be intermediate reaction products. After exposure in a hot furnace, mixtures of NaCl and acidic oxides with titanium yielded a large volume of gas having the color and odor of chlorine. In experiments in which pure NaBr and NaI were applied to titanium coupons, large quantities of free halogens were released on heating a few hours at 1100°F and so it was concluded that free chlorine was one of the reaction products in the former case. The formation of $TiCl_2$ was also deduced by observations made of the corrosion products. Corrosion pits were examined microscopically immediately after withdrawing Ti-6Al-4V samples in contact with NaCl for one hour at 850°F. A black substance was observed in the pits and it slowly turned to liquid and evolved a gas. It was concluded that the black substance was $TiCl_2$. $TiCl_2$ is a very dark purple solid that is extremely hygroscopic and reacts with water to evolve hydrogen. The final product is white titanium dioxide, which is consistent with the observations.

The suggested reactions are as follows:

I. $2NaCl + Ti + TiO_2 + 1/2O_2 = Na_2TiO_3 + TiCl_2$

II. $TiCl_2 + O_2 = TiO_2 + Cl_2$

III. $Ti + Cl_2 = TiCl_2$

Effect of alkali halides - Alkali halides are generally corrosive to titanium. The action of chlorides, bromides, and iodides suggests that the corrosion mechanism involves the formation of titanium halides and free halogens. Of the chlorides, LiCl was the most corrosive; KCl, NaCl and anhydrous $MgCl_2$ were about equal while $BaCl_2$ was the least corrosive.

Titanium Metallurgical Laboratory (4)

TML report #88 was compiled as the result of a symposium of Mallory-Sharon Titanium Corporation, Pratt and Whitney Aircraft, Rem-Cru Titanium, Inc., Republic Steel Corporation, and Titanium Metals Corporation of America.

Suggested reactions and thermodynamic probabilities - Evidence from thermodynamic considerations indicates the following chemical reactions may account for the high temperature sodium chloride corrosion of titanium. The chemical reactions discussed here were essentially those cited above with the addition of reaction 1a. The free energies for the reactions were calculated as follows:

		ΔF Kilocalories	
		440°F	1340°F
(1)a.	$2NaCl + Ti + O_2 = Na_2O_2 + TiCl_2$	-18.6	+0.9
b.	$2NaCl + Ti + TiO_2 + 1/2O_2 = Na_2TiO_3 + TiCl_2$	-47	-32
(2)	$TiCl_2 + O_2 + TiO_2 + Cl_2$	-106.4	-103.2
(3)	$Ti + Cl_2 = TiCl_2$	-97	-79

Armour Research Foundation (18)

Evidence of titanium dichloride - A diffraction pattern from scraping of a specimen corroded by a low-melting chloride salt mixture (LiCl-KCl eutectic) contained three lines which were in agreement with the strongest lines for $TiCl_2$.

Effect of stress on pure titanium in an atmosphere generally conducive to alloy cracking - Stress corrosion cracking was not observed in unalloyed titanium. (A similar study was conducted by MRL with similar results using sea-salt as the attacking agent.) Corrosion was not intergranular, but appeared to be more of a general nature with the occasional production of craters. Penetration in unalloyed titanium was several times greater for stressed specimens than for unstressed specimens.

Effect of anodizing - Anodizing affords Ti-6Al-4V little or no protection. Both freshly pickled and anodized bend specimens were exposed to 800°F for 48 hr in the presence of the following salts: LiCl-53KCl, NaCl-49$MgCl_2$, LiCl-34.9NaCl, KCl-70.5$BaCl_2$, and NaCl. Although the anodized films had an expected life of 1.8 years from the standpoint of dissolution, a considerable amount of penetration occurs making it evident that the film protection was lost by direct reaction with the salt. All of the above salts caused stress corrosion cracking.

Solubility of protective titania films in salt - TiO_2 protective films are dissolved by chloride salts. Various thicknesses of oxide films were anodized onto Ti-6Al-4V and were subsequently dissolved into a chloride salt at temperatures between 800°F and 1050°F. The resulting amount of dissolution of oxide into the salt was measured and with this data, diffusion coefficients at 800, 850, 900, 950, and 1000°F were determined to fit the equation

$$\Delta^2 = 0.613\ Dt + C$$

where

t = time

D = diffusion coefficient

Δ = decrease in the oxide film thickness,

and C = constant at each temperature.

It was proposed that, after the film elimination, NaCl reacts electrochemically to form $TiCl_2$ which disproportionates to form the tri- and tetrachlorides. These would depress the melting point of the salt layer adjacent to the metal to form a liquid salt mixture. The

corrosion rate is proportional to the amount of fused salt present.

M. E. Straumanis and Associates (11 through 14)

M. E. Straumanis and his co-workers found that titanium corrodes quickly in the presence of air and molten chlorides. When the oxygen concentration reaches 6.2 w/o, the surface layer breaks off and dissolves in the melt. This mechanism of the formation of pyrosols ($Ti + TiO_2$ in molten chlorides) continues as new surfaces of titanium are exposed to liquid salt and oxygen. Progressively less corrosion occurs in K, Na, and Li chloride melts.

Straumanis has suggested (19) that a similar phenomenon occurs in dry salt corrosion of titanium alloys.

Crucible Steel Company of America (8)

Thermodynamic considerations - The free energy changes for all of the reactions thought to be pertinent to this investigation were calculated for reactions of titanium with oxygen, chlorine, sodium chloride and titanium dioxide were calculated and graphed.

Role of acidic oxides in the absence of oxygen - Salt corrosion can be induced in the absence of oxygen if a reducible oxide is present. A mixture of TiO_2 and NaCl was welded in a one-inch thick block of Ti-5Al-2 1/2 Sn that was subsequently rolled at 1800°F to 1/4 inch and held for 100 hr at 900°F. Sectioning of the piece then showed the familiar corrosion product; however, an adjacent cavity (the control, containing only NaCl) indicated that sodium chloride alone will not react with titanium.

Presence of titanium monoxide - Titanium monoxide was identified by X-ray techniques. It was found generally in layers of salt closest to the metal surface. The following reactions may account for the typical characteristics of the reaction product on exposure to standard temperature and pressure:

$$TiCl_2 + (x + 1)\,H_2O = TiO \cdot x\,H_2O + 2\,HCl$$

$$TiO + (x+1)\,H_2O = TiO_2 \cdot x\,H_2O + H_2$$

Attempt to Identify Chlorine - Air was passed at a moderate rate through a Vycor tube containing a strip of titanium sheet coated

with sodium chloride. A tube furnace was used to heat the materials to about 1200°F. Chlorine was detected in the exit gas passed through a gas washing bottle containing potassium iodide. The color of liberated iodine intensified as the run progressed. Since control experiments were apparently not run here, however, one cannot be sure that the oxygen itself did not liberate the iodine.

Effect of air current - The formation of corrosion product is not altered by the direction of air flow. In a 65 hr test at 900°F, with an air flow of 2000 ml/minute being passed over a typical corrosion blister the formation of the corrosion product radiated concentrically about the salt, irrespective of the direction of wind velocity. This result was confirmed using inclined samples. Specimens suspended in a furnace for long periods of time showed greater attack at the top of the sample, however.

Evidence of a gaseous or vapor phase - Samples of titanium alloys were held above but not in direct contact with (a) mixtures of sodium chloride, titanium, and titanium dioxide, (b) mixtures of sodium chloride and titanium dioxide, and (c) sodium chloride for 24 hr at 1200°F and 65 hr at 900°F. Samples above (a) and (b) suffered the greatest attack as indicated by the amount of corrosion product on the surface of the sample. Samples above (c) did not show much greater attack than the samples exposed to air alone under the same conditions.

Effect of chlorine - Chlorine can cause stress corrosion cracking in the absence of air. Strips of Ti-12 Zr-7Al were bent into rings, stressing them beyond the yield point; they cracked on exposure for a few minutes at 500°F to air containing 1% chlorine. The experiment was repeated using 1% chlorine in argon, but the result was the same in both cases, i.e., the formation of intergranular cracks.

Effect of "sensitizing" treatment on pure titanium - Commercially pure titanium and super-alpha alloys can be sensitized to both aqueous stress corrosion cracking and to elevated temperature salt attack. Annealing pure titanium for six hours at 1900°F and longer caused failures in commercially pure titanium when stressed to 75 ksi in 5% HCl. Vulnerability is believed to be associated with preferential alloy and impurity partitioning and beta grain coarsening. Ti-12 Zr-7Al alloy was made susceptible to the same conditions after exposure for four hrs. at 1900°F. As a corollary to this effect, improved resistance to salt attack was obtained by laboratory processing at temperatures below the recrystallization temperatures.

Battelle Memorial Institute (16)

This work was compiled as a state-of-the-art report for NASA and refers to the most recent work done in the field of titanium stress corrosion research. Some of the data in the report was compiled from personal interviews and some from unpublished reports.

Effect of the dilute chloride solutions - Intergranular corrosion can be initiated from solutions containing as little as 100 ppm sodium chloride. In order to evaluate the effect of titanium exposure to chlorides prior to hot forming and hot sizing operations, distilled water containing 100, 200, 400, 600, or 1000 ppm sodium chloride was applied to the surface of titanium sheet specimens. Coupons 0.032 x 1 x 12 in. were bent in hoops having a 2 1/2 in. radius and were then subjected to air exposures at 1300°F for 1/2 hr.

The three alloys used in this study, Ti-7Al-12Cr, Ti-5Al-5Zr-Sn and Ti-8Al-1Mo-1V were all subject to cracking after the above treatment. Salt concentration of the order of 400 ppm are found in the tap water in San Diego.

Effect of oxygen enriched surfaces - Oxygen enrichment produces multiple surface-cracking when titanium is heated in air at elevated temperatures. Pratt and Whitney, along with their subcontractor shops, have reported the formation of brittle surface layers as a result of heating. The embrittlement was thought to be the result of interstitial absorption and varies depending on the alloy.

Effect of mechanical vibration and/or moving air - The lack of service failures imply that mechanical vibration and/or moving air may significantly retard the corrosion reaction. Accurate information regarding the precise conditions to which titanium alloys have been subjected in service is generally unavailable. A specific case, however, which is an outstanding example of titanium durability is cited in the following paragraph:

> "There are no special handling precautions in assembling the titanium compressor for the J93. Purple tints showing oxidation are found after exposure. Often fingermarks are outlined by the oxidation pattern. The vane received hot compressor air for anti-icing control at roughly 900°F. The velocity is of the order of 1000 ft per sec. No failures have been reported up to the present for this alloy under these severe conditions."

Effect of sea air exposure - Exposure to sea air is sufficient to induce vulnerability to stress corrosion cracking. Samples of titanium alloys that were exposed to sea air at El Segundo Beach were found to have the same vulnerability to cracking that specially salt coated samples had at Douglas and McDonnell.

Effect of alloying - Alloying has a significant effect on the resistance to cracking. Work done at the Langley Research Center (17) and at the Douglas Aircraft Company (18) indicate a relative susceptibility among the alloys. Ti-4Al-3Mo-1V, Ti-13V-11Cr-3Al, Ti-6Al-4V, Ti-8Al-1Mo-1V, and Ti-5Al-2.5Sn have been found to be vulnerable to stress corrosion cracking in that order. Under 100 ksi for 7000 hr at 550°F, Ti-4Al-3Mo-1V showed no embrittlement.

Effect of cycling temperature - Cycling from a hot dry salt environment to an aqueous room temperature bath does not eliminate susceptibility to cracking. At Boeing Aircraft (23) the effect of cycling bend specimens between a hot dry salt atmosphere at temperatures of 500, 550, and 600°F and a room temperature 3.5% NaCl dip are being made where the cyclic period is 60 minutes and the total test time is 1000 hr. No failures have been reported at 40 ksi and 500°F while at 550°F one sample failed in less than 1000 hr and the others showed serious property deterioration.

Effect of ozone - Ozone is recognized, thermodynamically, as being a greater threat in a hot salt atmosphere than any other reactant previously considered.